Multi-site, multi-crop measurements in the soil-vegetation-atmosphere continuum: A comprehensive dataset from two climatically contrasting regions in South West Germany for the period 2009-2018

5   Tobias K.D. Weber[1,*], Joachim Ingwersen[1], Petra Högy[2], Arne Poyda[1,a], Hans-Dieter Wizemann[3], Michael Scott Demyan[3,4,b], Kristina Bohm[1,c], Ravshan Eshonkulov[1,d], Sebastian Gayler[1], Pascal Kremer[1], Moritz Laub[3], Yvonne Funkuin Nkwain[2], Christian Troost[5], Irene Witte[1], Georg Cadisch[4], Torsten Müller[6], Andreas Fangmeier[2], Volker Wulfmeyer[3], Thilo Streck[1]

10   [1] Institute of Soil Science and Land Evaluation, University of Hohenheim, Stuttgart, Germany.

[2] Institute of Landscape and Plant Ecology, University of Hohenheim, Stuttgart, Germany

[3] Institute of Physics and Meteorology, University of Hohenheim, Stuttgart, Germany

[4] Institute of Agricultural Sciences in the Tropics, University of Hohenheim, Stuttgart, Germany

[5] Institute of Agricultural Sciences in the Tropics, University of Hohenheim, Stuttgart, Germany

15   [6] Institute of Crop Science, University of Hohenheim, Stuttgart, Germany

[a] current address: Institute of Crop Science and Plant Breeding, Grass and Forage Science / Organic Agriculture, Kiel University, Germany

[b] current address: School of Environment and Natural Resources, The Ohio State University, Columbus, Ohio, USA.

[c] previously published under the name Kristina Imukova

[d] current address: Karshi Engoneering-Economic Institute, Karshi, Uzbekistan

20   *Correspondence to:* Tobias KD Weber (tobias.weber@uni-hohenheim.de), Joachim Ingwersen (joachim.ingwersen@uni-hohenheim.de)

Keywords:

25   crop modelling, SVAT, eddy covariance, soil carbon, long-term observation, regional climate change, model calibration, crop phenology, Green Vegetation Fraction, GVF, LAI, Noah-MP; Land Surface Model, winter wheat, silage maize, winter rape, latent heat flux, sensible heat flux, ground heat flux, land-surface exchange, evapotranspiration

Abstract

We present a comprehensive, high-quality dataset characterising soil-vegetation and land-surface processes from continuous measurements conducted in two climatically contrasting study regions in South West Germany: the warmer and drier Kraichgau region with a mean temperature of 9.7°C and annual precipitation of 890 mm, and the cooler and wetter Swabian

5   Alp with mean temperature 7.5°C and annual precipitation 1042 mm. In each region, measurements were conducted over a time period of nine cropping seasons from 2009 to 2018. The backbone of the investigation was formed by six eddy-covariance stations (EC) which measured fluxes of water, energy and carbon dioxide between the land surface and the atmosphere at half-hourly resolution. This resulted in a dataset containing measurements from a total of 54 site*years containing observations with a multitude of crops, as well as considerable variation in local growing season climates.

10   The presented multi-site, multi-year data set is composed of crop-related data on phenological development stages, canopy height, leaf area index, vegetative and generative biomass and their respective carbon and nitrogen content. Time series of soil temperature and soil water content were monitored with 30-min resolution at various points in the soil profile, including ground heat fluxes. Moreover, more than 1,200 soil samples were taken to study changes of carbon and nitrogen contents. The data set was uploaded to the Pangaea database and can be accessed at https://doi.org/10.20387/bonares-a0qc-46jc (for the review

15   process, please refer to the data availability section). One station in each region has now been set up as continuous observatories of state variables and fluxes in intensively managed agricultural fields.

1 Introduction

It is well acknowledged that interactions between the soil-vegetation system and the atmosphere will have major impacts on regional climate and that our knowledge of processes and feedbacks is insufficient (Pielke et al., 2007, Thornton et al., 2014). Process models enable testing of hypotheses concerning the governing processes, identifying epistemic and aleatory

5 uncertainties and highlight the need for further investigations (Porter and Semenov, 2005, Godfray et al., 2010, Challinor et al., 2014, Tao et al., 2017, Schalge et al., 2020). Predicting the impacts of climate change on agroecosystems and land-surface exchange of water, energy, and momentum and, vice versa, requires process models to understand and study land-atmosphere feedbacks (Ingwersen et al., 2018, Monier et al., 2018). There is consensus that fully coupled climate, land surface, crop and hydrological models facilitate the prediction of climate change impacts on agricultural productivity as well as its feedbacks on

10 climate change projections themselves (Marland et al., 2003; Hansen, 2005; Perarnaud et al., 2005, Levis, 2010). This implies continuous improvement of models and process understanding. In relation to the water balance this includes, in particular, the partitioning of evaporation and transpiration (Kool et al., 2014, Stoy et al., 2019), modelling of crop transpiration (Heinlein et al., 2017), impacts on groundwater resources (Riedel and Weber, 2020), improving the representation of the Green Vegetation Fraction dynamics of croplands in Noah-MP Land Surface Model (Imukova et al., 2015, Bohm et al., 2019), dynamic root

15 growth of crops (Gayler et al., 2014) and assessing the relevance of subsurface processes (Gayler et al., 2013), evaluating the energy balance closure problem in eddy covariance measurements (Ingwersen et al., 2015, Imukova et al., 2016) and associated minor storage terms (Eshonkulov et al., 2019), as well as incorporating crop growth in land-surface models (Ingwersen et al., 2011, Ingwersen et al., 2018), investigating the carbon balance and turnover of agro-ecosystems (Demyan et al., 2016, Poyda et al., 2019), evaluating crop model performances (Bassu et al., 2014, Kimball et al., 2019), and response to changes in

20 environmental drivers (Biernath et al., 2011, Biernath et al., 2013) quantifying the effect of different intensities of free air carbon dioxide and temperatures on grain yield and grain quality (Högy et al., 2010, Högy et al., 2019), evaluating the worth of observed data (Wöhling et al., 2013b), and developing data-model integration techniques (Wöhling et al., 2013a).

However, the effects are further reaching than to biophysical environment. Regional climate projections typically neglect changes and adaptation of the agents of land use, namely the farmers, meaning that the concomitant projections of future crop

25 yields are based on crude simplifications (Hermans et al., 2010). Multi-agent system modelling has reached a level of maturity such that empirical bio-economic simulators can be run on high-performance computer clusters (Schreinemachers and Berger, 2011, Kelly et al., 2013). As a result, integrated model systems (Figure 1) can now be built that simulate both biophysical and socioeconomic processes with comparable process detail, accounting for the complex reality of local/regional human adaptation and feedback to global changes (Troost and Berger, 2015).

30 To enable an understanding of feedbacks within bioeconomic modelling systems, the models employed for the representation of processes of different complexity in the soil-vegetation-atmosphere continuum require calibration and validation against observed state variables or fluxes at the field level (Kersebaum et al., 2015). For this, high quality observed data on the state variables or fluxes of interest are required, which should encompass grain and biomass yields, soil organic carbon and nitrogen stocks and turnover in soils, as well as the water, carbon dioxide and energy fluxes between land surface and atmosphere. Still

35 very few model intercomparison studies include, in addition to crop growth, also soil water flux relevant variables to calibrate their agro-ecosystem models (Seidel et al., 2018), because data sets that include all these variables and fluxes are rare (Kersebaum et al., 2015). The dataset presented here is intended to help close this data gap, leading to better process representation on the one hand, while, on the other hand, facilitating model selection (Wöhling et al., 2015) and tackling the question of required and sufficient model complexity in the light of available data (Guthke, 2017).
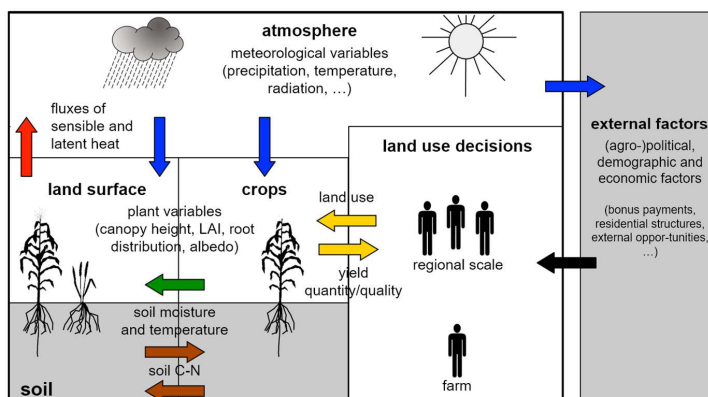
Figure 1 Diagram of the cardinal land modelling system compartments and relations. The presented dataset contains time series of quantified land surface, crops and soil processes and properties. This serves as a unique backbone for model validation and model development in soil-vegetation-atmosphere and robust land systems modelling.

5   To study the effects of regional climate change and to facilitate parameterisation and validation with the aim of continuous improvement of model components, extensive collaborative field measurements and controlled exposure experiments were carried out in two study areas in South West Germany. Both were intensively used agricultural landscape; 1) Kraichgau; mild climate, moderate precipitation, dominated by intensive row-crop agriculture, and 2) The Central Swabian Alb – *Mittlere Schwäbische Alb*; harsh climate, higher precipitation. Animal fattening, row crop agriculture, and heathland areas are important

10   features to the Central Swabian Alb agro-economic setting. Within the scope of this publication we present a high-quality dataset spanning a time period of nine cropping seasons from 2009 to 2018 intensely characterising the two respective agroecosystems. The backbone of the investigation was formed by six eddy-covariance stations which measured fluxes of water, energy and carbon dioxide between the land surface and the atmosphere at half-hourly resolution. This resulted in a dataset containing measurements from a total of 54 site*years (i.e. 2 regions * 3 fields * 9 cropping seasons) containing

15   observations with a multitude of crops, as well as considerable variation in local growing season climates. The data set comprises i) management and cultivation data (sowing date, harvest date, crop type and variety, fertilisation and pesticide application including amount and type (1-4 times per year), soil tillage, ii) plant performance (phenology, height, and leaf area index, with an average frequency of 7 observation times per year, yield (once per year^{-1}), above ground biomass (3-5 times per year), carbon and nitrogen in vegetative (sometimes separated in different plant compartments) and generative biomass, iii)

20   soil/biosphere-atmosphere fluxes using fully equipped eddy covariance stations for carbon, energy, and water vapor flux measurements as well as wind speed and wind direction aggregated to 30 min resolution (from 2009 to 2016 fluxes were not measured during the winter months), iv) soil characteristics, v) soil state measurements including water content, temperature, and matric potential (30 min), the soil profile permitting, at 5 cm, 15 cm, 45 cm, 75 cm, 90 cm, 130 cm soil depth, and vi) carbon and nitrogen measurements integrated over depths of 0-30 cm, 30-60 cm, 60-90 cm (4-6 times per year). In addition,

25   in selected years and at selected sites, green vegetation fraction measurements were performed, microbial carbon and nitrogen contents and CO_2 fluxes between the soil and the atmosphere were determined on vegetated and bare soil plots by means of the chamber method.
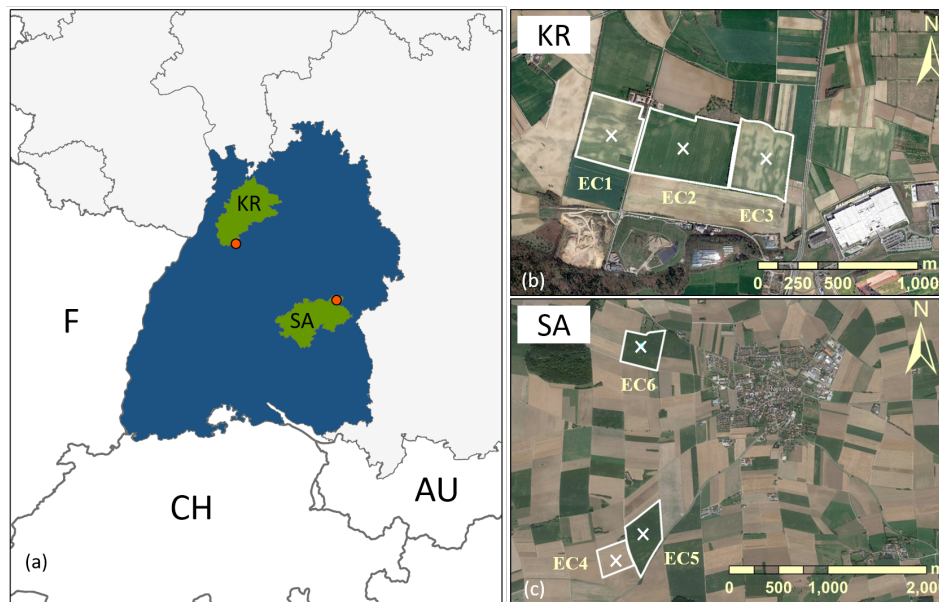
Figure 2: (a) Geographical overview and locations of the study sites and EC stations in (b) Kraichgau, KR and (c) Swabian Alb, SA (modified from Eshonkulov et al. (2019); © GoogleEarth Image: KR on 31 March 2017 and SA on 26 August 2016).

2 Material and Methods

5   In this section, the full dataset, which is composed of many individual datasets spanning diverse types of data sources, temporal and spatial measurement resolution, and origins, is individually described.

2.1 Site description

Measurements were performed in two research areas in two study regions, Kraichgau (48.92°N and 8.70°E, 319 m a.s.l.) and Central Swabian Alb (48.5°N and 9.8°E, 690 m a.s.l.). Each research area comprised three arable fields (in the following

10   research sites) managed by local farmers. Field research was part of the two wider integrated research projects PAK 346 *Structure and Function of Agricultural Landscapes under Global Climate Change – Processes and Projections on a Regional Scale* and RU 1695 *Agricultural Landscapes under Global Climate Change – Processes and Feedbacks on a Regional Scale*, funded by the German Research Foundation (DFG). While two research sites in both study regions (cf details below) were dismantled with completion of the research project in 2018, one research site in each region is still fully operational. In the

15   following, we give a detailed description of the study regions at large, and the research sites in particular. The study regions, research areas and study sites are shown in Figure 2.

Table 1 Soil characteristics at the three research sites EC1 to EC6.

EC	Ht	Hl	Hor	bd	por	fc	wp	stc	s	u	t	class	som	lc	pH
	cm	cm		g cm^{-3}	-	-	-	-	w-%	w-%	w-%		w-%	w-%	
	0	32	Ap	1.37	0.483	0.369	0.162	<1	2.5	79.4	18.1	Ut4	1.75	1.5	6.9
1	32	48	Sw-M	1.51	0.43	0.365	0.223	<1	2.0	79.2	18.8	Ut4	0.61	0.43	6.7
	48	>90	M-Sw	1.48	0.442	0.404	0.243	<1	0.9	80.4	18.7	Ut4	0.42	0.34	6.6
	0	33	Ap	1.33	0.498	0.343	0.153	<1	2.6	79.5	17.9	Ut4	1.53	1.38	6.2
2	33	72	Sw-M	1.46	0.449	0.371	0.223	<1	2.9	77	20.1	Ut4	0.52	0.43	6.4
	72	>90	M-Sw	1.53	0.423	0.417	0.239	<1	1.6	79.7	18.7	Ut4	0.34	0.28	6.5
	0	30	Ap	1.37	0.483	0.338	0.159	<1	1.8	81.1	17.1	Ut4	1.64	1.46	6.4
3	31	60	Sw-M	1.5	0.434	0.355	0.163	<1	1.0	80.4	18.6	Ut4	0.83	0.59	6.5
	60	>90	M-Sw	1.51	0.43	0.358	0.137	<1	0.8	83	16.1	Ut3	0.63	0.45	6.6
	0	21	Ap1	1.31	0.506	0.408	0.217	1_2	6.2	56	37.8	Tu3	4.35	3.2	6.9
4	21	29	Ap2	1.34	0.494	0.37	0.331	1_2	8.9	52.5	38.6	Tu3	2.13	2.04	6.8
	29	41	Tv	1.32	0.502	0.395	0.304	1_2	8.4	43.3	48.4	Tu2	1.63	1.37	6.7
	41	NA	cxC	NA	NA	NA	NA	>50	NA	NA	NA	NA	NA	NA	NA
	0	20	Ap	1.37	0.483	0.403	0.2	<1	2.8	68.3	28.9	Tu4	3.64	2.95	6.4
5	20	60	M1	1.4	0.472	0.335	0.21	<1	2.1	64.3	33.6	Tu3	1.44	1.4	6.4
	60	90	M2	1.51	0.43	0.417	0.302	<1	1.8	64	34.2	Tu3	0.71	0.56	6.2
	0	12	Ap1	1.04	0.608	0.384	0.228	2_5	3.2	51.2	45.6	Tu2	5.5	5.57	6.9
6	12	21	Ap2	1.29	0.513	0.422	0.228	5_10	4.1	48.3	47.6	Tu2	3.88	3.87	7.1
	21	NA	NA	NA	NA	NA	NA	NA	NA	NA	NA	NA	NA	NA	NA

EC: eddy covariance station, i.e. research site, Ht: top depth of soil horizon, Hl: lower depth of soil horizon, bd: bulk density, por: porosity, fc: field capacity, wp: wilting point, stc: stone content, S: sand, u: silts, t: clay, class: soil texture class, soil organic matter at the beginning of the research period in 2009, lc: lime content, w-%: weight percentage. The soil texture and texture classes are in reference to the German soil classification (Sponagel, 2005). Model parameters for the van Genuchten-Mualem soil hydraulic functions can be derived with a new pedotransfer function (Szabó et al., 2020), which includes uncertainties and the description of soil hydraulic properties over the full moisture range can be achieved using the Brunswick model (Weber et al., 2019, Streck and Weber, 2020) in conjunction with the pedotransfer function by Weber et al. (2020).

2.1.1 Kraichgau sites

The *Kraichgau* is a hilly region with fertile soils in the northwest of the state of Baden-Württemberg, SW Germany. It is part of the Neckar catchment and borders on the *Odenwald* low mountains in the north, the Neckar Valley in the northeast, the

5   *Stromberg* and *Heuchelberg* downlands in the Southeast, the Black Forest in the southwest and the Rhine Valley in the west. The natural geographic region of *Kraichgau* is located at an altitude of 100–400 m above sea level (a.s.l.) and covers approximately 1,600 km².

Due to its location in a basin surrounded by low mountain ranges, the Kraichgau is characterised by a mild climate with an annual mean temperature of more than 9°C making it one of the warmest regions in Germany. Mean annual precipitation

10   ranges from 720 to 830 mm, with a prevailing south-westerly wind direction. The central research area *Katharinenthalerhof* contains one ongoing research site. The research area is located close to the city of Pforzheim, SW Germany (48.92◦N, 8.70◦E). The area (385 m a.s.l.) is open and flat, and the prevailing wind direction is southwesterly. The parent soil material genesis is loess with a thickness of several metres. Because of temporally stagnant water conditions, particularly during spring, a Stagnic Regosol developed (World Reference Base for Soil Resources, WRB; Michéli et al., 2006). The underlying rock material is

15   shell limestone. The groundwater table is located more than 25 m below the surface. Three EC stations (EC1, EC2, and EC3) were installed at adjacent fields with the respective areas of 14.9, 23.6, and 15.8 ha (Figure 2): EC1 (48°55'42.60"N, 8°42'10.21"E) was in operation from 2009-04-16 to 2018-07-17, EC 2 (48°55'39.99"N, 8°42'32.03"E) from 2009-04-17 to

2018-10-29, and EC 3 (48°55'38.05"N, 8°42'57.37"E) from 2009-05-08 to 2018-09-17, dates indicate the time span of included measurements. Details on soil are provided in Table 1.

2.1.2 Swabian Alb sites

The low mountain range of Swabian Alb is a region with an approximate width of up to 40 km that stretches in a southwest-northeast direction over approximately 220 km, from the Black Forest in the Southwest to the Franconian Alb in the Northeast, covering an area of c. 5,700 km² in the state of Baden-Württemberg. To the northwest, the Swabian Alb is separated from the foothills by a 300–400 m high escarpment (*Albtrauf*). To the southeast, the Danube Valley forms the border to the geographic region of *Oberschwaben*. The Swabian Alb is structured in several geographic regions. Its central part is subdivided in the *Mittlere Kuppenalb* and the *Mittlere Flächenalb*. The *Mittlere Kuppenalb* in the northwest is characterised by mountains forming a hilly plateau which reaches elevations of 800–850 m a.s.l. The *Mittlere Flächenalb* in the south eastern part has a more levelled relief descending from about 650–750 m a.s.l. to the Danube Valley at about 520 m a.s.l. Due to its altitude, the climate of the *Kuppenalb* is much colder and harsher than that of the foothills. The mean temperature is 6-7 °C, i.e., lower by about 2 °C than in Kraichgau. Basins of cold air are typical for this cliffy karst region where night frost may occur even during summer months. Mean annual precipitation, which falls mostly during summer, ranges from 800 to 1,000 mm. Prevailing wind direction is westerly to southwesterly. Due to its lower elevation 'Flächenalb' is slightly warmer and drier (Troost and Berger, 2015).

The Swabian Alb is the largest contiguous karst region in Germany. The foothills are mostly formed by Black Jurassic and the escarpment by Brown Jurassic, whereas the plateau consists of White Jurassic. The in-situ unlayered reef limestones (*Massenkalke*) and dolomites are the reason for the deep karstification and the development of the hilly plateau crossed by widely ramified dry valleys. Depending on the bedrock, soils are clayey loams (*tonige Lehme*) and calcareous rendzinae (*Kalkscherbenböden*) or shallow calcareous black soils (*Kalkstein-Schwarzerden*), in the dry valleys decalcified loams.

The intensive agricultural land use in this area (Wöhling et al., 2013a) is characterized by a relatively balanced mix of crop production, dairy farming, bull fattening, pig production, and biogas production. Most farm holdings simultaneously produce three to five different crops, with spring barley, winter wheat, winter barley, and winter rapeseed being the dominant crops, while dairy and cattle farmers tend to also grow silage maize, clover, and field grass (Troost and Berger, 2015). The three research sites on Swabian Alb (*Flächenalb*) (Figure 2) have the coordinates: EC4 (48°31'38.95"N, 9°46'9.73"E, 685 m a.s.l.) was in operation from 2009-04-30 to 2018-08-31, EC5 (48°31'47.50"N, 9°46'23.41"E, 687 m a.s.l) from 2009-04-30 to 2018-08-02, and EC6 (48°32'49.29"N, 9°46'23.16"E, 692 m a.s.l.) from 2009-04-30 to 2018-07-26.

Table 2: Research sites EC1-6 and land use from 2010 to 2018.

| | | Kraichgau | | | Swabian Alb | | | | |
		EC1 14.9 ha	EC2 23.6 ha	EC3 15.8 ha	EC4 8.7 ha	EC5 16.7 ha	EC6 13.4 ha	Crop	Freq.
	2010	SM	WR	WW	WR	WW	CC-SM	CC-SM	13
	2011	WW	WW	CC-SM	WW	CC-SM	WW	SM	2
	2012	WR	CC-SM	WW	CC-SB	SM	WB	CC-GM	1
Year of Harvest	2013	WW	WW	WR	WR	WB	CC-SM	WW	22
	2014	CC-SM	CC-SM	WW	WW	SP	WW	SP	1
	2015	WW	WW	CC-SM	WW	CC-SM	WB	WB	5
	2016	CC-GM	WR	WW	CC-SB	CC-SM	CC-SM	CC-SB	2
	2017	WW	WW	WW	CC-SM	WB	WW	WR	8
	2018	WR	WW	CC-SM	WW	WR	WB	Sum	54

SM: silage maize, GM: grain maize, CC: cover crop, WW: winter wheat, WR: winter rapeseed, SP: spelt, WB: winter barley, SB: spring barley, Freq.: frequency

2.2 Field management and description

Basic field management information was provided by the farmers directly as field card index data. These contained information on crop rotations (Table 2), fertilization, soil management, and pesticide usage (Table 3). Crop yield is reported as total generative biomass at harvest by the farmers. Separately, vegetative and generative biomass was also determined by plot

5 sampling as part of the biomass characterization (c.f. 0). Under the assumption that no silage maize was used as fodder, that the water content of the harvested maize was 70% by mass, that the amount of carbon in the biogas digestate was 17.4% of the carbon exported from the field (Lindorfer and Frauz, 2015), and that the organic carbon content was 58% of Maize organic matter, we note the following: harvest and fertilization data provided by the farmers and included in the dataset, indicate that between the silage maize carbon exported and returned to the field with the biogas digestate, referenced to the 15 silage maize

10 cultivation periods, on average, approximately 900 kg ha^{-1} carbon were unaccounted for, indicating they may have been used as fertilisers, elsewhere. It is worth noting that the cover crops are not accounted for in the carbon balance.

From Table 3 it can be seen that the yields reported by the farmers are commonly lower than those reported by the scientists, which were determined at the experimental plots (cf. section 0). Very strong discrepancies of yields are found in the data of 2018 at EC2, EC4, and EC6, with inexplicably low yields reported for the plot replicates. In 2013, EC4 had a winter rapeseed

15 yield of 1.2 t ha^{-1}, which was attributed to hail damage.

Crop management was fairly typical for conventional intensive crop production in the areas. Noteworthy is the importance of biogas production, both as a motive for silage maize production and as a supplier of organic fertilizer. Choice of maize and wheat varieties in the sample reflects the climatic differences between the two locations. Due to the shorter growing season, early-maturing silage maize varieties (S220-S240) were preferred at the Swabian Alb sites, while the Kraichgau sites are

20 dominated by medium- to late-maturing varieties (S240-S310). With respect to winter wheat, the full spectrum of varieties ranging from hard (high protein/gluten, German classification group E) to soft (low protein, group C) varieties can be found. Wheat variety choice tends towards the higher quality end of the spectrum (groups E, A) in Kraichgau, and more towards the lower quality spectrum (groups B, C) in the Swabian Alb locations. Production of marketable quality wheat requires reliably favourable production conditions. Wheat yields are slightly higher (0.5 t) on average in the Swabian Alb, which may be a

25 consequence of the higher prevalence of the low protein wheat varieties (group B, C), which tend to have higher yields. The two spring barley yields reported by farmers are much higher (20-40%) than district averages for the respective years and considerably higher than typical spring barley yields in Germany. Similarly, winter barley yields on Swabian Alb research sites are about 20% higher than district averages. Silage maize and winter rapeseed yields at the Kraichgau research sites are in line with district averages. Silage maize yields on Swabian Alb are difficult to compare to district averages, as farmers

30 reported dry matter yields. Since the Central Swabian Alb lies at the margin of the maize suitability area, silage maize cannot always be harvested at a stage of ideal maturity and remaining water content cannot be assumed to always have reached literature values (this was not explicitly reported by the farmers). Hence any comparison with wet matter biomass observations reported at district levels is subject to considerable uncertainty and potential bias. In Table B-1 to Table B-3 we present average district yields for the crops of this study.

35 Table 3 indicates the number of pest and plant control operations between the harvest date of the previous crop and the harvest of the current crop. The number before the colon indicates the number of application, the upper case letters indicate the type of agent and the numbers in brackets the number applied agents applied. For example, at EC1 in 2010 herbicides were applied once, with three different agents. In the file plant_protection.csv, active substances of agent and application rates are further specified (cf. Table 3).

40

Table 3: Summary of field management and nutrient balance.

Site	Year	Crop[1] code	cultivar	group	Fertilization total N[2] and OM[3] input kg-N ha^{-1}	kg-C ha^{-1}	Pest and plant control[4] times and type	Yield[5] field Mg ha^{-1}	plot Mg ha^{-1}
EC1	2010	SM	Cannavaro	S310	29.2 (0)	0 (0)	1: H(3)	42.0	19.83 (2.38)
	2011	WW	Akteur	E	169.8 (169.8)	0 (0)	3: F(2),H(2)	8.41	10.25 (0.55)
	2012	WR	Elado_Artoga	-	210.5 (210.5)	0 (0)	3: F(1),H(3)	4.61	4.78 (0.44)
	2013	WW	Akteur	E	179.2 (179.2)	0 (0)	5: F(3),G(1),H(2)	8.64	8.86 (0.94)
	2014	CC-SM	Grosso	S250	51.2 (283)	0 (1767)	1: H(3)	52.6	23.24 (1.75)
	2015	WW	Sokal	A	265.8 (265.8)	349 (894)	3: F(3),G(1),H(3)	8.5	9.44 (1.58)
	2016	CC-GM	NAN	-	0 (219)	0 (0)	1: H(2)	11.0	14.06 (1.62)
	2017	WW	Patras	A	186 (186)	0 (0)	3: F(4),G(2),H(2),I(1)	7.8	8.21 (0.87)
	2018	WR	Alicante, Graf	-	373.4 (373.4)	968 (2482)	4: F(1),H(3),I(1)	4.2	4.31 (0.69)
EC2	2010	WR	NK Flair	-	268.1 (268.1)	0 (0)	1: F(1),I(1)	3.853	4.45 (0.2)
	2011	WW	Akteur	E	169.8 (169.8)	0 (0)	3: F(3),H(2)	8.95	9.44 (0.23)
	2012	CC-SM	Cannavaro	S310	109 (264)	0 (975)	1: H(3)	56.5	24.5 (1.4)
	2013	WW	Akteur	E	177.8 (177.8)	0 (0)	4: F(3),H(2)	7.65	7.91 (0.39)
	2014	CC-SM	Grosso	S250	210 (210)	0 (0)	1: H(3)	49.5	23.1 (1.25)
	2015	WW	Akteur	E	260.4 (260.4)	274 (702)	3: F(3),G(1),H(3)	8.7	10.15 (0.88)
	2016	WR	PR 46 W 26	-	173 (173)	0 (0)	3: F(1),H(4),I(1)	3.2	4.37 (0.97)
	2017	WW	Sokal	A	186 (186)	0 (0)	2: F(3),G(1),I(1)	9.2	9.5 (1.7)
	2018	WW	Patras, Sokal	A,A	185.7 (185.7)	0 (0)	3: F(2),G(2),H(2),I(1)	9.1	*2.6 (0.55)*[7]
EC3	2010	WW	Cubus	A	220.1 (220.1)	0 (0)	2: F(1),H(2),I(1)	7.11	7.95 (0.92)
	2011	CC-SM	Cannavaro	S310	40.5 (204)	0 (0)	1: H(3)	58.5	25.51 (1.85)
	2012	WW	Akteur	E	203.5 (203.5)	0 (0)	3: F(3),G(1),H(2),I(1)	7.82	9.94 (0.77)
	2013	WR	Alabaster, Fregat	-	235.1 (235.1)	0 (0)	3: F(1),H(2),I(1)	4.39	7.21 (0.58)
	2014	WW	JB Asano	A	198.2 (198.2)	0 (0)	2: F(2),H(1)	8.34	10.47 (1.15)
	2015	CC-SM	P 8509	-	138 (203)	0 (0)	2: H(3)	46.8	21.94 (2.15)
	2016	WW	Estivus Pamier Ferrum	A,A,B	206 (206)	0 (0)	2: F(3),G(3),H(2)	6.6	6.88 (0.93)
	2017	WW	Estivus	A	186 (186)	0 (0)	3: F(2),G(2),H(1),I(1)	6.0	6.21 (1.47)
	2018	CC-SM	various		0 (202)	0 (438)	1: H(3)	53.0	NA[8]
EC 4	2010	WR	Visby		210.9 (210.9)	0 (0)	6: F(4),G(2),H(4), I(3)	2.9	2.82 (0.53)
	2011	WW	Akteur	E	253 (253)	0 (0)	4: F(2),F(4),H(5),I(1)	8	8.33 (1.94)
	2012	CC-SB	Summer		65.5 (93.6)	0 (0)	3: F(3),H(3)	8.5	8.86 (0.36)
	2013	WR	PR 49 W 20		115.5 (133.5)	0 (0)	3: F(2),I(3)	1.2	1.83 (1.06)
	2014	WW	Orcas	B	202 (202)	0 (0)	2: G(1),H(2)	8.5	10.42 (0.41)
	2015	WW	Arezzo	B	226.5 (226.5)	0 (0)	3: F(3),G(1),H(1),I(1)	9.0	9.93 (0.97)
	2016	CC-SB	Grace		122.2 (289.4)	0 (0)	3: F(2),H(4)	8.1	6.22 (0.75)
	2017	CC-SM	LG 30 238	S220	114 (157)	3412 (1314)	2: H(2)	15*	30.6 (13.24)
	2018	WW	Porthus	B	195.7 (195.7)	341.6 (876)	3: F(4),G(2),H(3)	10.4	3.15 (0.27)
EC 5	2010	WW	Pamier	A	253 (253)	152.1 (390)	3: F(3),G(1),H(4)	7.9	9.05 (1.16)
	2011	CC-SM	Agro-Yoko	S240	206 (206)	138.5 (355)	1: H(2)	21	18.66 (1.6)
	2012	SM	Amanatidis	S220	97.4 (267.4)	0 (1065)	1: H(2)	17.2*	14.46 (1.72)
	2013	WB	Hobbit		270 (269.5)	249.2 (639)	3: F(3),G(1),H(2)	9.7	8.75 (0.29)
	2014	SP	Frankenkorn		170 (170)	276.9 (710)	2: F(1),G(1),H(2)	9.0	6.58 (1.12)
	2015	CC-SM	LG 30.217	S220	70.2 (162.2)	0 (0)	2: H(3)	16.2*	17.26 (2.64)
	2016	CC-SM	LG 30.217	S220	22.5 (151.3)	0 (0)	1: H(1)	17.4*	21.85 (1.52)
	2017	WB	Wotan	-	183 (183)	305 (781)	3: F(1),H(3)	8.9	10.46 (2.36)
	2018	WR	Bender	-	208 (308.4)	277 (1349)	2: H(2)	4.7	5.37 (1.03)
EC 6	2010	CC-SM	Fernandez, PR 39 A 98	S250, S240	90 (219)	0 (1110)	1: H(3)	13.8*	14.77 (3.07)
	2011	WW	Hermann	C	220.8 (220.8)	0 (0)	3: F(3),H(1)	8.88	9.49 (0.93)
	2012	WB	Winter		281.2 (281.2)	577.2 (1480)	2: F(3),G(1)	8.8	8.61 (1.29)
	2013	CC-SM	SY Kairo Agro-Yoko	S240, S210	127.5 (261)	585 (2055)	3: H(6)	NA	13.8 (2.32)
	2014	WW	Pamier	A	229.5 (229.5)	0 (0)	3: F(3),G(1),H(1)	9.9	9.3 (2.1)
	2015	WB	Amnisette	-	198.2 (198.2)	360.8 (925)	4: F(3),G(1),H(3)	7.2	8.37 (1.31)
	2016	CC-SM	Toninio	S230	151 (282.8)	398 (1576)	3: H(5)	18.0*	12.98 (2.81)
	2017	WW	Elixer	C	237 (237)	555 (1423)	5: F(3),G(3),H(4)	9.1	9 (0.82)
	2018	WB	California	-	206.7 (318.7)	415 (1917)	3: F(3),G(1),H(2)	7.8	1.78 (0.49)

1 SM: silage maize, GM: grain maize, CC: cover crop, WW: winter wheat, WR: winter rapeseed, SP: spelt, WB: winter barley, SB: spring barley, E, A, B, C,

2 applied N fertilizer amounts were reported as commercial products by the farmers. Subsequently, N_{tot}, $NH_4 - N$, $NO_3 - N$, and N_{amid} were calculated based on knowledge/estimates of respective N content in solid and liquid fertilizers. Numbers before brackets: Fertilised

amount between sowing and harvest and numbers in brackets fertilised amount between harvest of previous crop and harvest. The same was done for OM.
3 The total applied slurry (PS: pig slurry, CS: cow slurry, BS: biogas slurry) was reported by the farmer. The organic matter content was subsequently calculated based on a) laboratory analyses in 2015 and 2016 for KR, and 2014, 2015, and 2016 for research site EC6. Else, average values were assumed based on expert knowledge. More details can be found in the management metadata file.
4 H: herbicide, F: fungicide, I: Insecticide, GR: growth regulator. The number before ":" indicates the number of times plant control measures were undertaken on the field between the harvest date of the previous crop and the harvest date of the current crop. The numbers in brackets show the total number of product groups applied, where several may have been used at one application time.
5 Yield is reported as fresh mass of the generative biomass for all crops, except for SM where it relates to fresh mass of the total aboveground biomass reported by the farmer.
6 The low WR yield in 2013 was probably a consequence of damage due to hail.
7 Value is about three times lower than expected.
8 Last measured value before harvest was on 25 June (c.f. biomass.csv), NA: not available, *The silage maize yield at EC4-6 was reported as dry mass.

2.3 Field Measurements

All six EC stations were installed with the same instrumentation (Table 4, Table 5) for turbulent exchange (CSAT3, LI 7500), radiation (NR01), meteorological (HMP45, ARG 100) and soil measurements. CSAT3 and LI 7500 were installed 2–3 m
5   above the crop canopy and oriented in southern (KR) and south-western (SA) direction (specific details are given in the configuration histories, available in the data set). The stations were supplied by four 20 W solar panels. For the high-power consumption of the LI 7500 gas sensor, it had to be shut down during winter time, mainly from late November until March. In order to obtain results in winter time, EC2 and EC6 were each equipped with a fuel cell in autumn 2015. The HMP45 sensors were replaced by HC2S3 Hygroclip2 (Rotronic GmbH, Ettlingen, Germany) sensors at EC1 in December 2016, at EC2 in
10   September 2016, and at EC5 in 2017. At EC4 the HMP45 sensor was replaced by a new one end of August 2013. EC5 was shut down due to damage from August 2009 to May 2010 and from November 2011 to May 2012. The complete configuration histories of the EC stations are included in the datasets.

Table 4: Instrumentation of the eddy-covariance stations (Wizemann et al., 2015), occasional changes to the general layout are detailed in the text.

Sensor	Manufacturer	Model	Measurement Error (as given by the manufacturer)
Above-ground sensors			
3D Sonic Anemometer, Open path infrared H2O/CO2 Gas Analyzer (IRGA)	Campbell Scientific Inc., UK LI-COR Biosciences Inc., USA	CSAT3 LI7500	Horiz.: 1mm s⁻¹, vert.: 0.5mm s⁻¹ H2O (rms): ±3.3 mg m⁻³ at 10 Hz CO2 (rms): ±0.19 mg m⁻³ at 10 Hz Pressure: ±17 hPa
Radiation, 4-component*	Hukseflux Thermal Sensors, NL	NR01	SW: < 15 Wm⁻² at 1000 Wm⁻² LW: < 8 Wm⁻² at −100 Wm⁻² LWnet
Temperature, Relative Humidity	Vaisala Inc., Finland	HMP45	Temp.: ±0.3 °C, Hum.: ±2% RH
Rainfall	Environmental Measurements LTD, UK	ARG100	±2%
Soil sensors			
Temperature (up to 5)	Campbell Scientific Inc., UK	Model 107	< ±0.3 °C, typ. ±0.1 °C
TDR probes (up to 5)	Campbell Scientific Inc., UK	CS616	< 1.5% volumetric water content
Matric potential (up to 5)	Campbell Scientific Inc., UK	Model 253	
Heat flux plates (3)	Hukseflux Thermal Sensors, Netherlands	HFP01	±20 %, typ. ±10%
Logger			
Data logger	Campbell Scientific Inc., UK	CR3000, CR1000	

*SW: short wave, LW: long wave
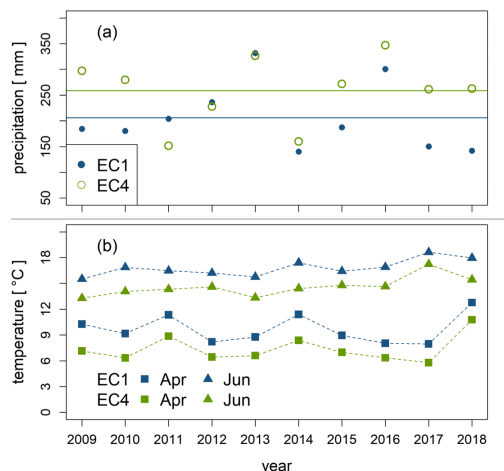
Figure 3: Selected meteorological variables at EC1 and EC4. Mean cumulative April-June precipitation, lines indicate the respective means. The years 2014, 2015 and 2018 show very dry growing season precipitation in KR (EC1) and in 2011, 2014 in SJ (EC 4). The difference in mean precipitation is 60 mm. (bottom) April and June mean air temperatures for 2009 to 2018. SJ is 2.2 (.5) °C cooler than KR. 2011, 2014, and 2018 showed very warm April months. The June temperature increases gradually from 2009 to 2018.

Table 5: Installation depths (in cm) of the soil sensors. During selected periods, additional sensors were installed in greater depths, particularly at EC1-3.

Sensor	EC1-3	EC4, EC5	EC6
Temperature	2, 6, 15, 30, 45	2, 6, 15, 30, 45	2, 6, 15, 30
TDR	5, 15, 30, 45, 75	5, 15, 30, 45	5, 15, 30
Matric potential	5, 15, 30, 45, 75	5, 15, 30, 45	5, 15, 30
Soil Heat Flux	8, three plates	8, three plates	8, three plates

2.3.1 Meteorological data

Meteorological data were measured at all eddy covariance stations and recorded on CR3000 data loggers (Campbell Scientific Inc., Logan, UT, USA) in 30 min intervals. Global radiation (Rg) and net radiation were measured with 4-component net radiometers (NR01, Hukseflux Thermal Sensors B.V., Delft, The Netherlands) that were installed about 1.5 m above the canopy. Air temperature (Ta) and humidity were measured in 2 m height (HMP45, Vaisala Inc., Helsinki, Finland; EC2 from September 2016 and EC1 from December 2016: HC2S3 Hygroclip2, Rotronic GmbH, Ettlingen, Germany) and precipitation in 1 m height (ARG100, EML, North Shields, UK). During the period 11 April – 2 November 2017, different sensors were used at EC1. During this time, long- and shortwave radiation was measured with a 4-component CNR4 net radiometer (Kipp & Zonen B.V., Delft, The Netherlands) and a HMP155 probe (Vaisala Inc., Helsinki, Finland) was used to measure air temperature and humidity. Data were stored on an XLite 9210 data logger (Sutron Corporation, Sterling, VA, USA). The convention used in this dataset is that all energy components directed away from the surface, are negative. April to June mean temperature and precipitation sum is presented in , which highlights the mean differences between the two regions. The inter-annual variability of precipitation is high, whereas that of temperature is low. Mean air June temperatures gradually increased over the reported 10 years. Rain and soil water content as well as soil temperature are shown as an example in Figure 5.

2.3.2 Surface-atmosphere fluxes

Surface-atmosphere fluxes (net CO_2 flux, sensible and latent heat flux) were measured with the eddy covariance (EC) technique. Each EC station was installed in the centre of a field (Figure 2) and equipped with a LI-7500 open path infrared CO_2/H_2O gas analyser (LI-COR Biosciences Inc., USA) and a CSAT3 3D sonic anemometer (Campbell Scientific Inc., UK). The measuring height was adjusted relative to the canopy height. The EC data were logged in 10 Hz resolution on a CR3000 data logger (Campbell Scientific Inc., Logan, UT, USA). All other sensor data were stored in 30 min intervals. At EC1, a different system was used during the period 11 April – 2 November 2017. During this time, this EC station was equipped with an LI-7200RS enclosed path CO2/H2O gas analyzer (LI-COR Biosciences, Lincoln, NE, USA) and a HS-50 3D-sonic anemometer (Gill Instruments Ltd., Hampshire, UK). Power supply for all EC stations was ensured by two solar-power batteries with capacities of 12 V and 250 Ah each (Keckeisen Akkumulatoren e.K., Memmingen, Germany). The batteries were charged by four 20 W solar panels (SP20, Campbell Scientific Inc., Logan, UT, USA) at each station. During periods with low solar altitude, however, the power supply was generally insufficient to ensure the operation of the LI-7500. For this reason, direct methanol fuel cell systems with 45 W maximum power supply (Efoy Pro 800 Duo, FSC Energy AG, Brunnthal-Nord, Germany) were installed at EC2 and EC6 in autumn 2015, enabling measurements of the surface-atmosphere fluxes at these locations also in winter.

The EC data from April 2009 to December 2012 were processed using the EC software package TK2, and after January 2013, version TK3.1 (Mauder and Foken, 2015). Fluxes were computed from 30 min covariances between vertical wind velocity and the corresponding scalar (CO_2 concentration, air temperature or humidity). In the TK software, we used the following settings: Spike detection (i.e., values exceeding 3.5 times the standard deviation of the last 10 values were labelled as spike), planar fit method for coordinate rotation with time periods between 7 to 12 days, Moore (1986) correction except for the longitudinal separation, which was taken into account by maximizing the covariances, Schotanus et al. (1983) procedure for converting the sonic into actual temperature, and density correction as suggested by Webb et al. (1980). For data quality analysis we used the nine-flag system of Foken (2006). Half-hourly fluxes with flag 7–9 (poor quality data) for friction velocity, sensible heat flux, or latent heat flux were excluded. For additional despiking of half-hourly fluxes, we applied a median filter using the median of absolute fluxes of the previous four days; fluxes that were > 5-times this median were discarded. For this, we used the R package REddyProc (Wutzler et al., 2020).

Data gaps occurred in times of sensor excavation for harvest and sowing, and due to browsing by animals. The stony ground at the SA sites made it necessary to install soil sensors at EC4 and EC5 at maximum in 45 cm depth and at EC6 in 15 cm depth. Time series of CO_2 fluxes are presented in Figure 4, by way of example, for EC1, and the data coverage for EC2-6 in the supporting information. On selected sites in some measurement campaigns, soil surface CO_2 chamber measurements were taken in both bare fallow and vegetated plots with EGM-2 and EGM-4 CO_2 detectors (PP Systems, Amesbury, MA) (Demyan et al., 2016).
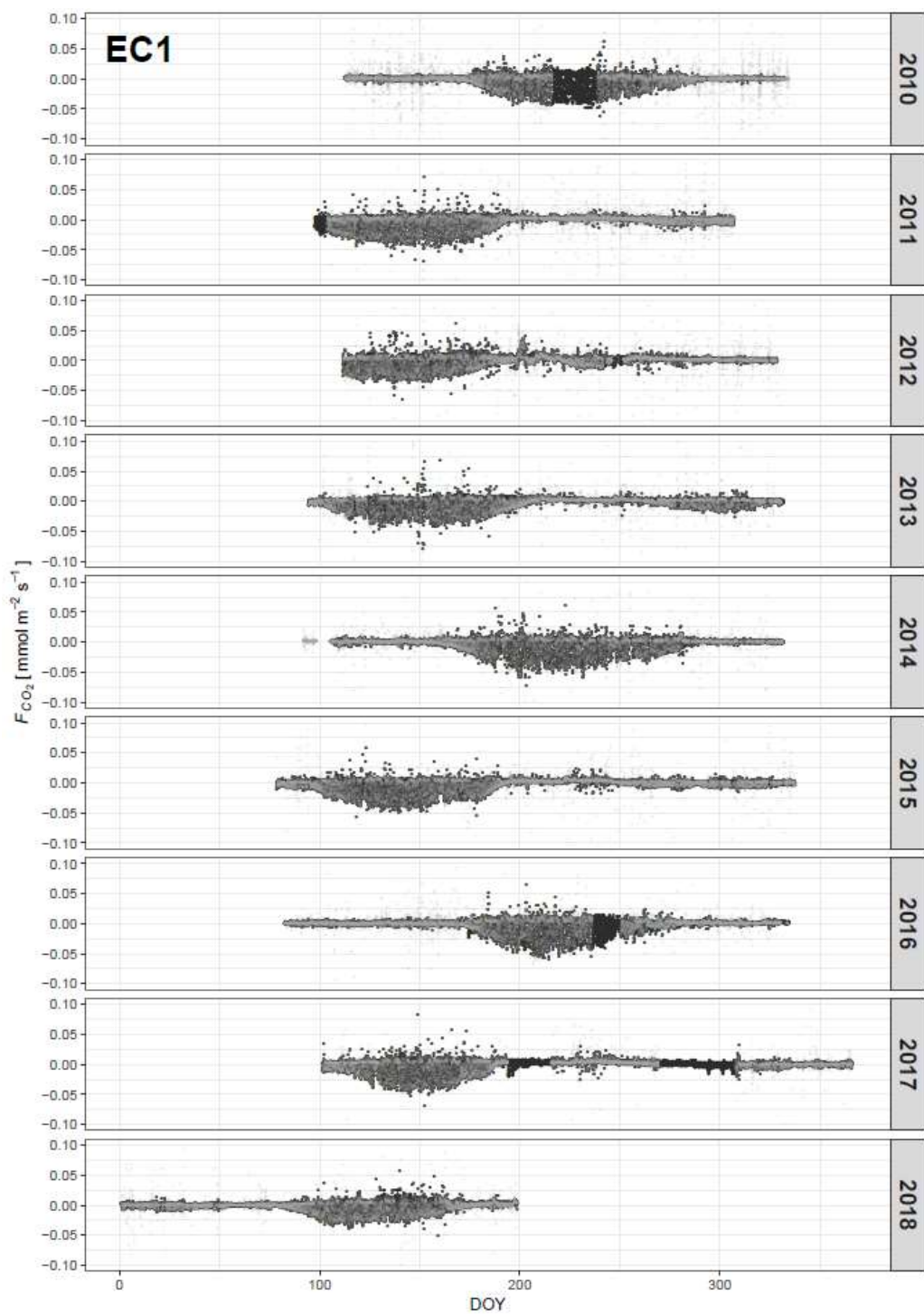
Figure 4: CO₂ fluxes measured by the eddy covariance method at EC1 for 2010-2018. Unfiltered measurements are depicted in grey and gap-filled data in black.
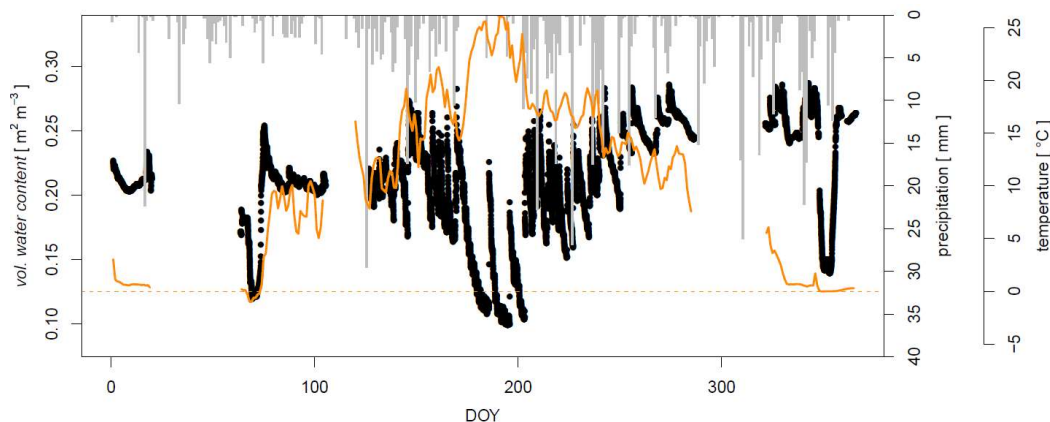
Figure 5: Soil water content (black dots), precipitation (grey bars), and soil temperature (orange line) at research site EC1 in 2010 at 5 cm soil depth. The dashed orange line indicates zero degree Celsius.

5   **2.3.3   Soil water content, soil heat fluxes, and soil temperature and matric potential measurements**

Adjacent to the EC stations, but in the tilled soil, temperature sensors (Model 107, Campbell Scientific Inc., UK) were installed in 2, 6, 15, 30 and 45 cm soil depth. To measure the volumetric soil water content and soil matric potential we installed FDR probes (CS616, Campbell Scientific Inc. UK) and matric potential sensors (Model 253, Campbell Scientific Inc., UK) in 5, 15, 30, 45 and 75 cm depth. Three soil heat flux plates (HFP01, Huskeflux Thermal Sensors, The Netherlands) were installed 8

10   cm below ground surface. At EC1, self-calibrating heat flux plates (HFP01SC, Campbell Scientific Inc., Logan, UT, USA) at 8 cm depth and HydraProbe II sensors (Stevens Water Monitoring Systems Inc., Portland, OR, USA) for soil volumetric water content and soil temperature at 5, 10 and 15 cm depth were used during the period 11 April – 2 November 2017. Soil water content and temperature at 5 cm depth and precipitation are presented in Figure 5 for EC1 in 2010, and Table 3where the strong drop in soil water contents around DOY 75 and DOY 350 are both attributed to soil freezing. We did not exclude

15   these data from our dataset intentionally. The remaining sites and years are presented in the

2.3.4   Phenological Development and Leaf Area Index

At each field, five plots of 4 m² were randomly selected and permanently marked to track phenological stage, reported on BBCH scale (Meier, 2018), total leaf area index, plant height, and plant biomass. Phenological stages were assessed at least in four-weekly intervals during winter and biweekly during the main growth period starting in autumn (winter crops) or early

20   spring (spring crops) until maturity. In 2017 and 2018, these measurements were carried out less frequently. During the main growth period starting in early spring, total leaf area index and plant height were determined about biweekly until crop maturity at the central square meter of every plot. A LAI-2000 Plant Canopy Analyzer (LI-COR Biosciences Inc., USA) was used to measure total leaf area index. Intermediate harvests of total aboveground biomass took place at stem elongation (decimal code (DC) 31 on BBCH scale) and full flowering (DC 65) using five extra plants per plot. At crop harvest (maturity), the biomass

25   of the central square meter of each subplot was cut at ground level and separated into vegetative and generative fractions. From 2017 on, also intermediate harvests were conducted on an areal basis. Biomass was sampled from 0.5 x 0.5 m² subplots for all crops except for maize, where plants were sampled from 1.5 m sections of the seeded rows and multiplied by row spaces for areal extrapolation.

2.3.5   Green Vegetation Fraction

For ground truth, Green Vegetation Fraction (GVF) was measured at EC1, EC2 and EC3 fields in 2012 and 2013 (Imukova et al., 2015). In 2012, winter rape (*Brassica napus* L. ssp. *napus*; cv. Artoga), silage maize (*Zea mays* L., cv. Cannavaro), and winter wheat (*Triticum aestivum* L. cv. Akteur) were cropped at EC1, EC2 and EC3, respectively. In 2013, at EC1 and EC2 winter wheat (*T. aestivum* L. cv. Akteur) and at EC3 winter rape (*B. napus* L. ssp. *napus* cv. Alabaster and Fregat) were grown. Within each study field, five plots (1 x 1 m^2) were permanently marked. During the growing season (April-October), canopy photos were taken from these plots in a weekly resolution. For the photos, a Nikon COOLPIX P7000 digital camera (Nikon Corporation, Tokyo, Japan) was used. Photos were taken from one meter above the canopy (nadir sampling) using the automatic mode of the camera, with and without flash. The photos are available as part of the dataset. This measurement campaign was extended by using RapidEye satellite images were used to derive high-resolution gridded GVF data (cell grid size of 5×5 m^2). Satellite images were provided by the German Aerospace Center (DLR) as a part of the RapidEye Science Archive (proposal 505). Obtained high-resolution GVF grid data revealed a bimodal distribution of GVF at the regional scale during the growing seasons (Imukova et al. 2015). This bimodal behaviour is explained by phenological differences between early covering (ECC: ex., winter wheat, winter rape etc.) and late covering crops (LCC: ex., maize, sugar beet). Our results imply splitting the generic cropland class of Noah-MP into ECC and LCC has the potential to improve the simulation of energy and water fluxes at the land surface, particularly during the second part of the growing season (Bohm et al. 2020).

2.4   Field Sampling

Soil sampling

To determine total and mineral nitrogen (NH$_4^+$, NO$_3^-$) and organic carbon, soil samples were taken at least in spring (March/April) and autumn (October/November) from the depths 0-30, 30-60 and 60-90 cm at all six research sites during almost all years. Two replicate samples were taken at five permanent locations at every site. In November 2017, soil bulk density was determined at the six research sites (EC1-6) using cylinders with 4 cm height and 100 cm³ volume. Undisturbed cores were taken from depths 0-4, 13-17, 26-30, 36-40 and 46-50 cm if this was possible, depending on soil thickness and stone content. Prior to gravimetric measurement of the water content, soil cores were stored air-tight. For the determination of dry weight, samples were dried at 105°C until constant weight.

Additional bare-fallow plots were established in 2009, 2010 and 2012 (bare09, bare10, bare12, respectively, presented in separate files), at each research site (EC1-6). Plots were kept clear of vegetation during the experiment by manual weeding and periodic spot spraying of glyphosate (Monsanto Agrar, GmbH, Germany). Vegetated plots were tilled by hand in a way as to mimic mechanized tillage. In addition to plant residues, the vegetated plots received manure/slurry and mineral fertilizer as organic inputs. Samples were collected from 0 – 30 and 30 – 60 cm in bare fallow and vegetated plots in addition from 60 – 90 cm depth on vegetated plots. Due to the shallow soil at EC6, samples were collected at 30 cm depth. Composite soil samples were prepared by mixing five soil cores taken within a specific area in each plot into one homogenous sample. Total organic C (TOC) and N, soil microbial biomass, and soil respiration were monitored four times per year.

Plant sampling

To track phenological development, at each research site crop samples were taken at the five permanent locations mentioned above. Intermediate harvests were performed at stem elongation (DC 31 according to BBCH scale) and full flowering (DC 65) using five extra plants per plot. At crop maturity, the aboveground biomass of the central square meter of each plot was harvested (final harvest).

2.5 Laboratory measurements

2.5.1 Soil organic carbon and nitrogen

Soil microbial biomass C and N (C_{mic} and N_{mic}) analyses were conducted on wet samples using the chloroform-fumigation-extraction (CFE) method (Joergensen, 1996). Briefly, approximately 20 g non-sieved soil samples were fumigated with

5   ethanol-free chloroform for 24 hours. Fumigated and non-fumigated samples were extracted with 0.5M K_2SO_4 solution. C_{mic} and N_{mic} in extracts were analysed with a Multi N/C analyser (Analytik Jena AG, Jena, Germany). Mineral N (ammonium and nitrate) was measured in the non-fumigated 0.5 M K_2SO_4 extracts using a flow-injection analyser (FIAstar 5000, FOSS, Denmark). C_{mic} and N_{mic} were calculated from the difference in C and N contents of fumigated and non-fumigated samples using a k_{EC} value of 0.45 and a k_{EN} value of 0.54 (Joergensen, 1996) after correcting for gravimetric moisture content. Total

10   organic C (TOC) in bulk soil was analysed by dry combustion according to DIN ISO 13878 (1998) with a Vario-EL III elemental analyser (Elementar, Hanau, Germany).The soil samples from vegetated plots were analyzed for organic carbon and total nitrogen content (vario MACRO cube, Elementar Analysensysteme GmbH) as well as for ammonium and nitrate concentrations. Ammonium was determined photometrically in a Nitroprussid-Salicylat solution. Nitrate was measured by ion chromatography (861 Advanced Compact IC, Metrohm) equipped with an anion separation column (Metrosen A supp5,

15   Metrohm). Gravimetric moisture content was determined by drying approximately 0.1 kg of wet soil at 105 °C for 24 hours.

2.5.2 Plant carbon and nitrogen content

Plant material was separated into vegetative and generative fractions. Vegetative parts were dried to constant weight at 60 °C, generative parts at 28 °C. After determining dry weights generative parts were manually threshed to determine crop yield whereas the vegetative parts were cut using a chaff cutter and homogeneously mixed. Randomly picked material of vegetative

20   parts and of harvestable products was milled using a laboratory mixer mill (MM 301, Retsch, Haan, Germany). Fine powder of vegetative parts and of harvestable products were analysed for carbon and nitrogen using an elemental analyser (Vario EL, Elementar Analysensysteme, Hanau, Germany) as described in Högy et al. (2009). In 2017 and 2018 the residual water content was determined, too. This was achieved by further oven drying of the samples at 105 °C until a constant weight had been reached.

25   ## 3 Scope and structure of the dataset

We provide figures and tables alluding to the scope and nature of the data sets. The data set is structured as described in Figure 6. The intent is to provide an overview of the quantified system variables and properties, without needless repetition of previously peer-reviewed analyses. In view of the fact that the dataset contains 17 sub-datasets, the structure is presented here explicitly. All data files were ensured to be machine-readable using the software *R*, and the library *data.table* and function

30   *fread*. The column names, units, data types and descriptors are listed in Table 7 - Table 19 (*for the review process, Table 7 - Table 19 are found in section 12*). Numerous figures with time series of the flux and soil measurements are presented in the Supplementary Information.

35

```
Structure of the dataset
    ./__gis                | geo-location of research sites and plots.
                             The keys 'site' and 'plot' link the data sets.

    ./00_metadata          | information on the data sets

    ./01_ec_flux           | eddy covariance station data

    ./02_chamber_fluxes    | weather data (model drivers)

    ./03_weather           | water content

    ./04_soil              | weather data (model drivers)

    ./05_management        | model drivers, e.g. farm management
        /cultivation       |   sowing, harvest and info on Wheat varieties
        /fertilization     |   C and N-input
        /soil_management   |   model input

    ./06_plant             | observations of plant data
        /biomass           |   time series of biomass of plants
        /cn                |   C/N ratios of plant samples
        /lai               |   leaf area index
        /phenology         |   phenological development

    ./07_soil_properties   | observation of soil data
        /cn                |   time series of CN measurements
        /profile           |   soil profile description

    ./08_GVF               | empty, please refer to seperate data publication
```

Figure 6: Folder structure of the dataset.

4   Data availability

The combined digital database is available freely for download from https://doi.org/10.20387/bonares-a0qc-46jc. For the review process, the datasets can be downloaded https://b-web.bonares.de/smartEditor/rest/upload/for1695_data.zip (full dataset without the photos of the green vegetation fraction approx. 150 Mb), and the images are available under

5   https://b-web.bonares.de/smartEditor/rest/upload/for1695_data_GVF.zip (images of the green vegetation fraction approx. 2750 Mb). These links are replaced by the doi, after the publication process.

5   Summary and conclusion

We provide a comprehensive data set on agricultural crop growth and land surface exchange on arable soils in Germany. The continuous eddy covariance measurements on adjacent fields and the long duration of our measurements (2009-2018) is unique

10   and allows for new insights into the role of crop rotations for land surface exchange processes. According to a recent report by the Alliance of Science Organisations in Germany our installations have been the only ones on agricultural land throughout South Germany that fulfil the criteria for becoming part of the intended national observatory network for terrestrial ecosystem research (Kögel-Knabner et al., 2018).

We recognized that the interannual variability within locations exceeds the effect of regional climate. In other words, a direct

15   comparison of fluxes measured in the two study regions are only possible if the measurements are performed in the same year under comparable large scale weather conditions (Wizemann et al., 2015). Although some dryer growing seasons were identified with sometimes low soil volumetric water contents in the upper soil layers, it became apparent that the deep loess soil profiles in the Kraichgau region and the soils in the cooler and wetter Swabian Alb region were generally not severely water-deficient. An exception to that was the very early ripening and subsequently harvest of maize in the Kraichgau region

20   in 2018.

The dataset was used extensively to calibrate soil-crop models and land-surface models. In spite of the high data quality and the extensive coverage of crops and years, we would like to draw the attention on some possible improvements to future campaigns like the one presented. First, it became apparent that it would be beneficial to include measurements to infer information on the partitioning between evaporation and transpiration of the crops. Also, we notice that, due to solar power

25   shortage in winter, we have some data gaps in the EC measurements. We think it would be worthwhile to extend the research by extending the measurements on soil (hydraulic) properties (transience, hydrophobicity, structure …). In the future, it would be beneficial to properly quantify the contribution of the cover crops to the overall fluxes and budgets, as well as to include

sensors that capture the N$_2$O emission. Extending the monitoring of root growth as well as of root water uptake and root decay by more detailed, continuous measurements would very valuable for model improvement. Finally, we note that the measurements will be continued at the two research sites EC2 and EC4, that is, at one site in each region.

6 Appendix A

Table A-1: Further information on the quantification rules to calculate the amount and type of mineral N from the reported applied mineral fertilizers on the 54 site*years and the organic matter (OM) content.

Fertiliser type	Density	N_{total}	$NO_3 - N$	$NH_4 - N$	N_{amid}	type
	kg L^{-1}	%	%	%	%	-
Ammonium sulfate solution	1.25	15	3.5	8.6	2.9	liquid
Ammon nitrate urea solution	1.28	28	7	7	14	liquid
Piasan	1.31	25	5	9	11	liquid
Calcium ammonium nitrate	na	27	13.5	13.5	na	solid
NPK	na	rv	$0.5 * N_{total}$	$0.5 * N_{total}$	na	solid
Urea/Alzon	na	rv or 46	na	na	rv or 46	solid
Ammonium Sulphate Nitrate	na	21	15.5	5.5	na	solid
Piamon 33 S	na	33	na	10.4	22.6	solid
InnoFert	na	24	7.8	16.2	na	solid

na: not applicable, rv: reported value

Table A-2: Further information on the quantification rules to calculate the amount and type of mineral N from the reported applied mineral fertilizers on the 54 site*years and the organic matter (OM) content.

Fertiliser type	TS	OM	N_{total}	$NH_4 - N$
	%	%	%	%
Biogas slurry	6	73	0.43	0.26
Cow slurry	8	71	0.39	0.21
Pig slurry	5	71	0.56	0.42

TS: total solids, OM: organic matter
Nutrient contents determined in the laboratory in 2015 and 2016 for Kraichgau and 2014, 2015, and 2016 for research site EC6 (SA). Otherwise, average values were assumed based on expert knowledge, as given below

7 Appendix B

Table B-1: Average yields of the Kraichgau district Enzkreis for the years 2010-2018. Non available values are indicated by NA.

Kraichgau - Enzkreis	2010	2011	2012	2013	2014	2015	2016	2017	2018	Average
						Mg ha-1				
Winter wheat	6.72	7.74	7.38	7.35	7.08	8.3	6.62	7.78	8.04	7.4
Winter barley	6.45	6.1	6.92	6.82	7.04	7.05	6.21	7.46	7.17	6.8
Spring barley	5.03	5.36	6.28	4.84	NA	5.35	NA	NA	NA	4.5
Oat	4.53	NA	NA	NA	NA	5.13	NA	NA	NA	4.8
Triticale	5.66	NA	NA	NA	NA	NA	NA	NA	NA	5.7
Grain maize	9.54	NA	NA	NA	NA	NA	8.82	10.34	9.93	9.7
Potatoes	31.51	NA	NA	NA	NA	NA	NA	NA	NA	31.5

Sugar beat	0	NA	NA	NA	NA	NA	NA	NA	NA	NA
Winter rapeseed	3.8	3.3	3.5	3.7	5.2	4.5	3.6	4.3	4.2	4.0
Silage maize	43.9	56.9	51.4	42.1	57.6	42.7	42.3	43.3	NA	47.5

Table B-2: Average yields of the Swabian Jura district Alb-Donau for the years 2010-2018. Non available values are indicated by NA.

Swabian Jura Alb-Donau-Kreis	2010	2011	2012	2013	2014	2015	2016	2017	2018	Average
						Mg ha^{-1}				
Winter wheat	7.2	8.1	7.6	7.97	8.56	7.95	7.11	8.09	8.13	7.9
Winter barley	6.21	7.18	7.22	7.13	7.68	6.78	6.77	7.44	6.83	7.0
Spring barley	5.51	6.23	6.87	5.86	6.35	5.61	5.68	5.28	5.76	5.9
Oat	5.07	4.56	6.35	5.29	5.44	NA	4.84	5.04	NA	5.2
Triticale	6.95	8.13	7.75	8.28	8.75	7.67	6.19	7.55	7.03	7.6
Grain maize	10.04	10.85	11.31	10.38	NA	9.04	9.52	8.2	8.79	9.8
Potatoes	34.62	41.01	55.88	25.65	NA	38.56	46.49	42.05	37.9	40.3
Sugar beat	71.06	75.3	79.33	NA	NA	NA	65.19	NA	65.46	71.3
Winter rapeseed	3.76	3.46	4.19	4.04	5.1	4	3.87	3.94	4.14	4.1
Silage maize	45.81	46.58	50.27	41.79	48.56	38.13	48.01	47.54	45.16	45.8

5   **Table B-3: Average yields of the Swabian Jura district Reutlingen for the years 2010-2018. Non available values are indicated by NA.**

Swabian Jura Reutlingen	2010	2011	2012	2013	2014	2015	2016	2017	2018	Average
						Mg ha-1				
Winter wheat	6.29	6.53	6.29	5.51	7.19	5.92	5.87	6.64	7.06	6.4
Winter barley	6.06	6.38	5.82	5.5	7.69	5.97	6.33	6.93	6.74	6.4
Spring barley	4.87	5.31	5.38	4.39	6.35	4.56	3.76	4.95	5.26	5.0
Oat	4.72	5.3	5.82	5.1	5.9	4.62	4.92	3.99	NA	5.0
Triticale	6.4	6.71	7.3	6.73	6.38	6.14	5.19	6.15	6.67	6.4
Grain maize	NA	NA	NA	NA	NA	NA	NA	NA	NA	NA
Potatoes	28.2	31.85	27.49	20.33	29.39	15.4	7.03	23.25	27.21	23.4
Sugar beat	NA	NA	NA	NA	NA	NA	NA	NA	NA	NA
Winter rapeseed	3.65	NA	3.89	2.88	NA	NA	NA	3.48	3.84	3.5
Silage maize	35.81	41.46	41.55	35.85	NA	31.48	32.91	35	34.93	36.1

8   Author Contribution

TW: Tobias Weber, JI: Joachim Ingwersen, PH: Petra Högy: AP: Arne Poyda, HDW: Hans-Dieter Wizemann, PK: Pascal Kremer, IW: Irene Witte, RE: Ravshan Eshonkulov, KB: Kristina Bohm, ML: Moritz Laub, MSD: Scott Demyan, GC: Georg Cadisch, TM: Torsten Müller, AF: Andreas Fangmeier, VW: Volker Wulfmeyer, TS: Thilo Streck, CT: Christian Troost, YFN: Yvonne Funkuin Nkwain

Table 6: Author contributions.

code	Topic	Details	Contributors (Initials)
1	Conceptualization	Ideas; formulation or evolution of overarching research goals and aims.	GC, PH, TS
2	Data curation	Management activities to annotate (produce metadata), scrub data and maintain research data (including software code, where it is necessary for interpreting the data itself) for initial use and later re-use.	TW, CT, HDW, PH, ML, YFN, MSD, AP, PK, JI
3	Formal analysis	Application of statistical, mathematical, computational, or other formal techniques to analyse or synthesize study data.	TW, HDW, PH, AP, PK
4	Funding acquisition	Acquisition of the financial support for the project leading to this publication.	TM, AF, GC, PH, JI, VW, TS
5	Investigation	Conducting a research and investigation process, specifically performing the experiments, or data/evidence collection.	KB, HDW, TW, RE, PH, YFN, ML, MSD, AP, PK, TS
6	Methodology	Development or design of methodology; creation of models.	TM, PH, TS, JI
7	Project administration	Management and coordination responsibility for the research activity planning and execution.	PH, VW, TS, JI
8	Resources	Provision of study materials, reagents, materials, patients, laboratory samples, animals, instrumentation, computing resources, or other analysis tools.	TM, GC, PH, AF, JI, TS
9	Software	Programming, software development; designing computer programs; implementation of the computer code and supporting algorithms; testing of existing code components.	TW, GC, HDW, JI
10	Supervision	Oversight and leadership responsibility for the research activity planning and execution, including mentorship external to the core team.	TM, GC, PH, AP, JI, VW, TS
11	Validation	Verification, whether as a part of the activity or separate, of the overall replication/reproducibility of results/experiments and other research outputs.	TW, CT, KB, PH, AP, PK, JI
12	Visualization	Preparation, creation and/or presentation of the published work, specifically visualization/data presentation.	TW, PH, JI
13	Writing – original draft	Preparation, creation and/or presentation of the published work, specifically writing the initial draft (including substantive translation).	TW, PH, YFN, ML, AP, JI
14	Writing – review & editing	Preparation, creation and/or presentation of the published work by those from the original research group, specifically critical review, commentary or revision – including pre- or post-publication stages.	TW, TM, CT, AP, JI, PH, TS, MSD

9   Competing interests

None of the authors declare a conflict in interest.

10   Acknowledgements

This data set is the result of the DFG (German Research Foundation) Integrated Project PAK 346 *Structure and Functions of Agricultural Landscapes under Global Climate Change - Processes and Projections on a Regional Scale*, and the DFG funded Research Unit 1695 *Agricultural Landscapes under Global Climate Change - Processes and Feedbacks on a Regional Scale*. TW was funded by the Collaborative Research Center 1253 CAMPOS (Project 7: Stochastic Modelling Framework), funded by the German Research Foundation (DFG, Grant Agreement SFB 1253/1 2017). We specifically acknowledge the distinguished farmers who enabled this research, namely Mr. Bosch senior (†) and Mr Bosch junior (EC1-EC3), Mr Fink (EC4), Mr Hermann (EC5), and Mr. Reichert (EC6), further, the technical staff team members B. Prechter and T. Schreiber, and student helpers: F. Baur and C. Schade. KB was financed by a scholarship in the frame of the Erasmus Mundus IAMONET-RU program. The authors are grateful to Dr. W. Damsohn, G. Gensheimer, Dr. Z. Kauf, Mr Strohm, and the students for

assistance at the field experiments. Parts of this study were funded by the Federal Ministry of Education and Research (01PL11003), Humboldt Reloaded Projects at the University of Hohenheim, Germany. Lastly, we thank Dr. A. Klumpp and Prof. Dr. J. Auerbacher for their support.

11 References

5 Bassu, S., Brisson, N., Durand, J.-L., Boote, K., Lizaso, J., Jones, J. W., Rosenzweig, C., Ruane, A. C., Adam, M., Baron, C., Basso, B., Biernath, C., Boogaard, H., Conijn, S., Corbeels, M., Deryng, D., Sanctis, G. de, Gayler, S., Grassini, P., Hatfield, J., Hoek, S., Izaurralde, C., Jongschaap, R., Kemanian, A. R., Kersebaum, K. C., Kim, S.-H., Kumar, N. S., Makowski, D., Müller, C., Nendel, C., Priesack, E., Pravia, M. V., Sau, F., Shcherbak, I., Tao, F., Teixeira, E., Timlin, D., and Waha, K.: How do various maize crop models vary in their responses to climate change factors?, Global Change
10 Biology, 20, 2301–2320, doi:10.1111/gcb.12520, 2014.

Biernath, C., Bittner, S., Klein, C., Gayler, S., Hentschel, R., Hoffmann, P., Högy, P., Fangmeier, A., and Priesack, E.: Modeling acclimation of leaf photosynthesis to atmospheric CO_2 enrichment, European Journal of Agronomy, 48, 74–87, doi:10.1016/j.eja.2013.02.008, 2013.

Biernath, C., Gayler, S., Bittner, S., Klein, C., Högy, P., Fangmeier, A., and Priesack, E.: Evaluating the ability of four crop
15 models to predict different environmental impacts on spring wheat grown in open-top chambers, European Journal of Agronomy, 35, 71–82, doi:10.1016/j.eja.2011.04.001, 2011.

Bohm, K., Ingwersen, J., Milovac, J., and Streck, T.: Distinguishing between early and late covering crops in the land surface model Noah-MP: Impact on simulated surface energy fluxes and temperature, 2019.

Challinor, A. J., Watson, J., Lobell, D. B., Howden, S. M., Smith, D. R., and Chhetri, N.: A meta-analysis of crop yield
20 under climate change and adaptation, Nature Clim Change, 4, 287–291, doi:10.1038/nclimate2153, 2014.

de Vries, D. A.: Thermal properties of soils, in: Physics of Plant Environment, van Wijk, W. R. (Ed.), North-Holland Publishing Company, Amsterdam, 210–235, 1963.

Demyan, M. S., Ingwersen, J., Funkuin, Y. N., Ali, R. S., Mirzaeitalarposhti, R., Rasche, F., Poll, C., Müller, T., Streck, T., Kandeler, E., and Cadisch, G.: Partitioning of ecosystem respiration in winter wheat and silage maize—modeling
25 seasonal temperature effects, Agriculture, Ecosystems & Environment, 224, 131–144, doi:10.1016/j.agee.2016.03.039, 2016.

Eshonkulov, R., Poyda, A., Ingwersen, J., Wizemann, H.-D., Weber, T. K. D., Kremer, P., Högy, P., Pulatov, A., and Streck, T.: Evaluating multi-year, multi-site data on the energy balance closure of eddy-covariance flux measurements at cropland sites in southwestern Germany, Biogeosciences, 16, 521–540, doi:10.5194/bg-16-521-2019, 2019.

30 Foken, T.: Angewandte Meteorologie: Mikrometeorologische Methoden, Zweite, überarbeitete und erweiterte Auflage, Springer-Verlag Berlin Heidelberg, Berlin, Heidelberg, 2006.

Gayler, S., Ingwersen, J., Priesack, E., Wöhling, T., Wulfmeyer, V., and Streck, T.: Assessing the relevance of subsurface processes for the simulation of evapotranspiration and soil moisture dynamics with CLM3.5: comparison with field data and crop model simulations, Environ Earth Sci, 69, 415–427, doi:10.1007/s12665-013-2309-z, 2013.

35 Gayler, S., Wöhling, T., Grzeschik, M., Ingwersen, J., Wizemann, H.-D., Warrach-Sagi, K., Högy, P., Attinger, S., Streck, T., and Wulfmeyer, V.: Incorporating dynamic root growth enhances the performance of Noah-MP at two contrasting winter wheat field sites, Water Resour. Res., 50, 1337–1356, doi:10.1002/2013WR014634, 2014.

Godfray, H. C. J., Beddington, J. R., Crute, I. R., Haddad, L., Lawrence, D., Muir, J. F., Pretty, J., Robinson, S., Thomas, S. M., and Toulmin, C.: Food security: the challenge of feeding 9 billion people, Science (New York, N.Y.), 327, 812–818,
40 doi:10.1126/science.1185383, 2010.

Guthke, A.: Defensible Model Complexity: A Call for Data-Based and Goal-Oriented Model Choice, Ground Water, 55, 646–650, doi:10.1111/gwat.12554, 2017.

Hansen, J. W.: Integrating seasonal climate prediction and agricultural models for insights into agricultural practice, Philosophical Transactions of the Royal Society B: Biological Sciences, 360, 2037–2047, doi:10.1098/rstb.2005.1747, 2005.

Heinlein, F., Biernath, C., Klein, C., Thieme, C., and Priesack, E.: Evaluation of Simulated Transpiration from Maize Plants on Lysimeters, Vadose Zone Journal, 16, 0, doi:10.2136/vzj2016.05.0042, 2017.

Hermans, C., Geijzendorffer, I. R., Ewert, F., Metzger, M. J., Vereijken, P. H., Woltjer, G. B., and Verhagen, A.: Exploring the future of European crop production in a liberalised market, with specific consideration of climate change and the regional competitiveness, Ecological Modelling, 221, 2177–2187, doi:10.1016/j.ecolmodel.2010.03.021, 2010.

Högy, P., Franzaring, J., Schwadorf, K., Breuer, J., Schütze, W., and Fangmeier, A.: Effects of free-air CO2 enrichment on energy traits and seed quality of oilseed rape, Agriculture, Ecosystems & Environment, 139, 239–244, doi:10.1016/j.agee.2010.08.009, 2010.

Högy, P., Kottmann, L., Schmid, I., and Fangmeier, A.: Heat, wheat and CO 2 The relevance of timing and the mode of temperature stress on biomass and yield, J Agro Crop Sci, 205, 608–615, doi:10.1111/jac.12345, 2019.

Högy, P., Wieser, H., Köhler, P., Schwadorf, K., Breuer, J., Franzaring, J., Muntifering, R., and Fangmeier, A.: Effects of elevated CO2 on grain yield and quality of wheat: results from a 3-year free-air CO2 enrichment experiment, Plant biology (Stuttgart, Germany), 11 Suppl 1, 60–69, doi:10.1111/j.1438-8677.2009.00230.x, 2009.

Imukova, K., Ingwersen, J., Hevart, M., and Streck, T.: Energy balance closure on a winter wheat stand: comparing the eddy covariance technique with the soil water balance method, Biogeosciences, 13, 63–75, doi:10.5194/bg-13-63-2016, 2016.

Imukova, K., Ingwersen, J., and Streck, T.: Determining the spatial and temporal dynamics of the green vegetation fraction of croplands using high-resolution RapidEye satellite images, Agricultural and Forest Meteorology, 206, 113–123, doi:10.1016/j.agrformet.2015.03.003, 2015.

Ingwersen, J., Högy, P., Wizemann, H. D., Warrach-Sagi, K., and Streck, T.: Coupling the land surface model Noah-MP with the generic crop growth model Gecros: Model description, calibration and validation, Agricultural and Forest Meteorology, 262, 322–339, doi:10.1016/j.agrformet.2018.06.023, 2018.

Ingwersen, J., Imukova, K., Högy, P., and Streck, T.: On the use of the post-closure methods uncertainty band to evaluate the performance of land surface models against eddy covariance flux data, Biogeosciences, 12, 2311–2326, doi:10.5194/bg-12-2311-2015, 2015.

Ingwersen, J., Steffens, K., Högy, P., Warrach-Sagi, K., Zhunusbayeva, D., Poltoradnev, M., Gäbler, R., Wizemann, H.-D., Fangmeier, A., Wulfmeyer, V., and Streck, T.: Comparison of Noah simulations with eddy covariance and soil water measurements at a winter wheat stand, Agricultural and Forest Meteorology, 151, 345–355, doi:10.1016/j.agrformet.2010.11.010, 2011.

Joergensen, R. G.: The fumigation-extraction method to estimate soil microbial biomass: Calibration of the kEC value, Soil Biology and Biochemistry, 28, 25–31, doi:10.1016/0038-0717(95)00102-6, 1996.

Kelly, R. A., Jakeman, A. J., Barreteau, O., Borsuk, M. E., ElSawah, S., Hamilton, S. H., Henriksen, H. J., Kuikka, S., Maier, H. R., Rizzoli, A. E., van Delden, H., and Voinov, A. A.: Selecting among five common modelling approaches for integrated environmental assessment and management, Environmental Modelling & Software, 47, 159–181, doi:10.1016/j.envsoft.2013.05.005, 2013.

Kersebaum, K. C., Boote, K. J., Jorgenson, J. S., Nendel, C., Bindi, M., Frühauf, C., Gaiser, T., Hoogenboom, G., Kollas, C., Olesen, J. E., Rötter, R. P., Ruget, F., Thorburn, P. J., Trnka, M., and Wegehenkel, M.: Analysis and classification of

data sets for calibration and validation of agro-ecosystem models, Environmental Modelling & Software, 72, 402–417, doi:10.1016/j.envsoft.2015.05.009, 2015.

Kimball, B. A., Boote, K. J., Hatfield, J. L., Ahuja, L. R., Stockle, C., Archontoulis, S., Baron, C., Basso, B., Bertuzzi, P., Constantin, J., Deryng, D., Dumont, B., Durand, J.-L., Ewert, F., Gaiser, T., Gayler, S., Hoffmann, M. P., Jiang, Q.,

5   Kim, S.-H., Lizaso, J., Moulin, S., Nendel, C., Parker, P., Palosuo, T., Priesack, E., Qi, Z., Srivastava, A., Stella, T., Tao, F., Thorp, K. R., Timlin, D., Twine, T. E., Webber, H., Willaume, M., and Williams, K.: Simulation of maize evapotranspiration: An inter-comparison among 29 maize models, Agricultural and Forest Meteorology, 271, 264–284, doi:10.1016/j.agrformet.2019.02.037, 2019.

Kögel-Knabner, I., Teutsch, G., Adrian, R., Blanckenburg, F., Flügge, U.-I., Kolle, O., Kleinn, C., Küsel, K., Lischeid, G.,

10   Löw, A., Schäfers, C., Schmid, H., Simmer, C., Vereecken, H., Walz, R., Haase, P., Lütkemeier, E., Weymann, D., Brüchmann, C., and Ute, W.: Empfehlung zur Einrichtung eines nationalen Observatorien-Netzes für die terrestrische Ökosystemforschung: Abschlussbericht der Arbeitsgruppe „Infrastrukturen in der terrestrischen Forschung" der Allianz der Wissenschaftsorganisationen, 2018.

Kool, D., Agam, N., Lazarovitch, N., Heitman, J. L., Sauer, T. J., and Ben-Gal, A.: A review of approaches for

15   evapotranspiration partitioning, Agricultural and Forest Meteorology, 184, 56–70, doi:10.1016/j.agrformet.2013.09.003, 2014.

Lasslop, G., Reichstein, M., Papale, D., Richardson, A. D., ARNETH, A., BARR, A., Stoy, P., and WOHLFAHRT, G.: Separation of net ecosystem exchange into assimilation and respiration using a light response curve approach: critical issues and global evaluation, Global Change Biol, 16, 187–208, doi:10.1111/j.1365-2486.2009.02041.x, 2010.

20 Levis, S.: Modeling vegetation and land use in models of the Earth System, WIREs Clim Change, 1, 840–856, doi:10.1002/wcc.83, 2010.

Lindorfer, H. and Frauz, B.: Biogas Biorefineries, in: Industrial Biorefineries & White Biotechnology, Elsevier, 271–294, 2015.

Marland, G., Pielke, R. A., Apps, M., Avissar, R., Betts, R. A., Davis, K. J., Frumhoff, P. C., Jackson, S. T., Joyce, L. A.,

25   Kauppi, P., Katzenberger, J., MacDicken, K. G., Neilson, R. P., Niles, J. O., Niyogi, D. d. S., Norby, R. J., Pena, N., Sampson, N., and Xue, Y.: The climatic impacts of land surface change and carbon management, and the implications for climate-change mitigation policy, Climate Policy, 3, 149–157, doi:10.3763/cpol.2003.0318, 2003.

Mauder, M. and Foken, T.: Documentation and Instruction Manual of the Eddy-Covariance Software Package TK3 (update), Arbeitsergebnisse, Bayreuth, 62, 2015.

30 Meier, U.: Growth stages of mono- and dicotyledonous plants: BBCH Monograph, Open Agrar Repositorium, 2018.

Michéli, E., Schad, P., and Spaargaren, O.: World reference base for soil resources 2006: A framework for international classification, correlation and communication, World soil resources reports, 103, Food and agriculture organization of the United nations (FAO), Rome, 128 pp., 2006.

Monier, E., Paltsev, S., Sokolov, A., Chen, Y.-H. H., Gao, X., Ejaz, Q., Couzo, E., Schlosser, C. A., Dutkiewicz, S., Fant, C.,

35   Scott, J., Kicklighter, D., Morris, J., Jacoby, H., Prinn, R., and Haigh, M.: Toward a consistent modeling framework to assess multi-sectoral climate impacts, Nature communications, 9, 660, doi:10.1038/s41467-018-02984-9, 2018.

Moore, C. J.: Frequency response corrections for eddy correlation systems, Boundary-Layer Meteorol, 37, 17–35, doi:10.1007/BF00122754, 1986.

Perarnaud, V., Seguin, B., Malezieux, E., Deque, M., and Loustau, D.: Agrometeorological Research and Applications

40   Needed to Prepare Agriculture and Forestry to 21st Century Climate Change, Climatic Change, 70, 319–340, doi:10.1007/s10584-005-5953-9, 2005.

Pielke, R. A., Adegoke, J., BeltraáN-Przekurat, A., Hiemstra, C. A., Lin, J., Nair, U. S., Niyogi, D., and Nobis, T. E.: An overview of regional land-use and land-cover impacts on rainfall, Tellus B: Chemical and Physical Meteorology, 59, 587–601, doi:10.1111/j.1600-0889.2007.00251.x, 2007.

Porter, J. R. and Semenov, M. A.: Crop responses to climatic variation, Philosophical Transactions of the Royal Society B: Biological Sciences, 360, 2021–2035, doi:10.1098/rstb.2005.1752, 2005.

Poyda, A., Wizemann, H.-D., Ingwersen, J., Eshonkulov, R., Högy, P., Demyan, M. S., Kremer, P., Wulfmeyer, V., and Streck, T.: Carbon fluxes and budgets of intensive crop rotations in two regional climates of southwest Germany, Agriculture, Ecosystems & Environment, 276, 31–46, doi:10.1016/j.agee.2019.02.011, 2019.

Reichstein, M., Falge, E., Baldocchi, D., Papale, D., Aubinet, M., Berbigier, P., Bernhofer, C., Buchmann, N., Gilmanov, T., Granier, A., Grunwald, T., Havrankova, K., Ilvesniemi, H., Janous, D., Knohl, A., Laurila, T., Lohila, A., Loustau, D., Matteucci, G., Meyers, T., Miglietta, F., Ourcival, J.-M., Pumpanen, J., Rambal, S., Rotenberg, E., Sanz, M., Tenhunen, J., Seufert, G., Vaccari, F., Vesala, T., Yakir, D., and Valentini, R.: On the separation of net ecosystem exchange into assimilation and ecosystem respiration: review and improved algorithm, Global Change Biol, 11, 1424–1439, doi:10.1111/j.1365-2486.2005.001002.x, 2005.

Riedel, T. and Weber, T. K. D.: The influence of global change on Europe´s water cycle and groundwater recharge, Hydrogeology Journal, accepted, 2020.

Schalge, B., Baroni, G., Haese, B., Erdal, D., Geppert, G., Saavedra, P., Haefliger, V., Vereecken, H., Attinger, S., Kunstmann, H., Cirpka, O. A., Ament, F., Kollet, S., Neuweiler, I., Hendricks Franssen, H.-J., and Simmer, C.: Presentation and discussion of the high resolution atmosphere-land surface subsurface simulation dataset of the virtual Neckar catchment for the period 2007–2015, 2020.

Schotanus, P., Nieuwstadt, F., and Bruin, H. de: Temperature measurement with a sonic anemometer and its application to heat and moisture fluxes, Boundary-Layer Meteorol, 26, 81–93, doi:10.1007/BF00164332, 1983.

Schreinemachers, P. and Berger, T.: An agent-based simulation model of human–environment interactions in agricultural systems, Environmental Modelling & Software, 26, 845–859, doi:10.1016/j.envsoft.2011.02.004, 2011.

Seidel, S. J., Palosuo, T., Thorburn, P., and Wallach, D.: Towards improved calibration of crop models – Where are we now and where should we go?, European Journal of Agronomy, 94, 25–35, doi:10.1016/j.eja.2018.01.006, 2018.

Sponagel, H.: Bodenkundliche Kartieranleitung: Mit 103 Tabellen, 5., verb. und erw. Aufl., Schweizerbart, Stuttgart, 438 S., 2005.

Stoy, P. C., El-Madany, T. S., Fisher, J. B., Gentine, P., Gerken, T., Good, S. P., Klosterhalfen, A., Liu, S., Miralles, D. G., Perez-Priego, O., Rigden, A. J., Skaggs, T. H., WOHLFAHRT, G., Anderson, R. G., Coenders-Gerrits, A. M. J., Jung, M., Maes, W. H., Mammarella, I., Mauder, M., Migliavacca, M., Nelson, J. A., Poyatos, R., Reichstein, M., Scott, R. L., and Wolf, S.: Reviews and syntheses: Turning the challenges of partitioning ecosystem evaporation and transpiration into opportunities, Biogeosciences, 16, 3747–3775, doi:10.5194/bg-16-3747-2019, 2019.

Streck, T. and Weber, T. K. D.: Analytical expressions for noncapillary soil water retention based on popular capillary retention models, Vadose Zone J., 2020.

Szabó, B., Weynants, M., and Weber, T. K. D.: Updated European hydraulic pedotransfer functions with communicated uncertainties in the predicted variables (euptfv2), doi:10.5194/gmd-2020-36, 2020.

Tao, F., Rötter, R. P., Palosuo, T., Gregorio Hernández Díaz-Ambrona, C., Mínguez, M. I., Semenov, M. A., Kersebaum, K. C., Nendel, C., Specka, X., Hoffmann, H., Ewert, F., Dambreville, A., Martre, P., Rodríguez, L., Ruiz-Ramos, M., Gaiser, T., Höhn, J. G., Salo, T., Ferrise, R., Bindi, M., Cammarano, D., and Schulman, A. H.: Contribution of crop model structure, parameters and climate projections to uncertainty in climate change impact assessments, Global Change Biol, doi:10.1111/gcb.14019, 2017.

Thornton, P. K., Ericksen, P. J., Herrero, M., and Challinor, A. J.: Climate variability and vulnerability to climate change: a review, Global Change Biol, 20, 3313–3328, doi:10.1111/gcb.12581, 2014.

Troost, C. and Berger, T.: Dealing with Uncertainty in Agent-Based Simulation: Farm-Level Modeling of Adaptation to Climate Change in Southwest Germany, American Journal of Agricultural Economics, 97, 833–854,
5   doi:10.1093/ajae/aau076, 2015.

Webb, E. K., Pearman, G. I., and Leuning, R.: Correction of flux measurements for density effects due to heat and water vapour transfer, Q.J Royal Met. Soc., 106, 85–100, doi:10.1002/qj.49710644707, 1980.

Weber, T. K., Durner, W., Streck, T., and Diamantopoulos, E.: A modular framework for modelling unsaturated soil hydraulic properties over the full moisture range, Water Resour. Res., doi:10.1029/2018WR024584, 2019.

10   Weber, T. K. D., Finkel, M., Conceição Gonçalves, M., Vereecken, H., and Diamantopoulos, E.: Pedotransfer function for the Brunswick soil hydraulic property model and comparison to the van Genuchten-Mualem model, Water Resour Res, doi:10.1029/2019WR026820, 2020.

Weber, T. K. D., Ingwersen, J., Högy, P., Poyda, A., Wizemann, H-D, Demyan, M. S. Bohm, K., Eshonkulov, R., Gayler, S., Kremer, P., Laub, M., Nkwain, Y. F., Troost, C., Witte, I., Cadisch, G., Müller, T., Fangmeier, A., Wulfmeyer, V., and
15   Streck, T., Multi-site, multi-crop measurements in the soil-vegetation-atmosphere continuum: A comprehensive dataset from two climatically contrasting regions in South West Germany for the period 2009-2018, doi: 10.20387/bonares-a0qc-46jc, 2021 (under internal review, please refer to data availability section for the discussion).

Wizemann, H.-D., Ingwersen, J., Högy, P., Warrach-Sagi, K., Streck, T., and Wulfmeyer, V.: Three year observations of water vapor and energy fluxes over agricultural crops in two regional climates of Southwest Germany, metz, 24, 39–59,
20   doi:10.1127/metz/2014/0618, 2015.

Wöhling, T., Gayler, S., Priesack, E., Ingwersen, J., Wizemann, H.-D., Högy, P., Cuntz, M., Attinger, S., Wulfmeyer, V., and Streck, T.: Multiresponse, multiobjective calibration as a diagnostic tool to compare accuracy and structural limitations of five coupled soil-plant models and CLM3.5, Water Resour. Res., 49, 8200–8221, doi:10.1002/2013WR014536, 2013a.

25   Wöhling, T., Geiges, A., Nowak, W., Gayler, S., Högy, P., and Wizemann, H. D.: Towards Optimizing Experiments for Maximum-confidence Model Selection between Different Soil-plant Models, Procedia Environmental Sciences, 19, 514–523, doi:10.1016/j.proenv.2013.06.058, 2013b.

Wöhling, T., Schöniger, A., Gayler, S., and Nowak, W.: Bayesian model averaging to explore the worth of data for soil-plant model selection and prediction, Water resources research, 51, 2825–2846, doi:10.1002/2014WR016292, 2015.

30   Wutzler, T., Reichstein, M., Moffat, A. M., and Migliavacca, M.: REddyProc: Post Processing of (Half-)Hourly Eddy-Covariance Measurements: https://CRAN.R-project.org/package=REddyProc, 2020.

12   Tables of Section 3

Table 7: Variables and description of the field cultivation data files (cultivation.csv) including farmer reported yield.

Column Name	Unit	Description
site	-	field name
sdate	YYYY-MM-DDThh:mm	sowing date
hdate	YYYY-MM-DDThh:mm	harvest date
crop	-	cultivated crop
var	-	crop variety
code	-	crop code (used throughout the database)
sdens	-	seed density of sown crop
unit	seed m^{-2}; kg ha^{-1}	unit of seed density, sdens
yield	t ha^{-1}	yield as reported by the farmer
ref	DM o. FM	reference mass of the yield (referenced to dry matter weight of fresh matter weight)
residue	%	percent of residues left after harvest

5   **Table 8: Variables and description of the soil management data files (soil_management.csv).**

Column Name	Unit	Description
site	-	field name
date	YYYY-MM-DDThh:mm	date of soil management
Depth	m	depth of soil management
Type	-	type of soil management
Code	-	abbreviation for Expert-N (Priesack, 2006)

Table 9: Determined variables and description of the soil carbon and nitrogen measurement files (soil_cn.csv).

Column Name	Unit	Description
site	-	field name
date	YYYY-MM-DDThh:mm	measurement date
plot	-	plot number
depth	cm	indicator of soil layer depth: 30 | soil layer 0-30 cm depth, 60 | soil layer 30-60 cm depth, 90 | soil layer 60-90 cm depth
bd	g cm^{-3}	bulk density of the soil sample
no3N	mg kg^{-1}	nitrate-N (no3N)
nh4N	mg kg^{-1}	ammonium-N (nh4N)
soc	mg kg^{-1}	total soil organic carbon
son	mg kg^{-1}	total soil organic nitrogen
cmic	mg kg^{-1}	soil microbial carbon
nmic	mg kg^{-1}	soil microbial nitrogen
sub_plot_type	-	"veg" - vegetated, and "b09", "b10", "b12" - bare plots in the years 2009, 2010, 2012

Table 10: Determined variables and description of the fertilizer data files (fertilization.csv).

Column Name	Unit	Description
site	-	field name
date	YYYY-MM-DDThh:mm	application date
FE_farm	-	fertilizer as reported by the farmer
FE_com	-	common name of fertilizer (full name)
FE_type	min; org	mineral (min) or organic (org) fertilizer
FE_code	ssiii	fertilizer code (as used by Expert-N (Priesack, 2006))
quantity	-	quantity of applied fertilizer
unit	kg ha^{-1}; m^3 ha^{-1}; L ha^{-1}; t ha^{-1}	unit of the applied fertilizer
DM	kg ha^{-1}	calculated dry matter in the applied organic fertilizer
OM	kg ha^{-1}	calculated organic matter in the applied organic fertilizer
N	kg ha^{-1}	total quantity of N in the applied fertilizer
nh4N	kg ha^{-1}	quantity of ammonium-N in applied fertilizer
no3N	kg ha^{-1}	quantity of nitrate-N in applied fertilizer
amidN	kg ha^{-1}	quantity of amidN in applied fertilizer

The farmers reported type and total amount of applied fertilizer type. Based on information provided from the fertiliser suppliers, analyses on the organic matter content of the organic fertilizers (slurry) and selected gap filling by expert knowledge, the data set can be considered complete. However, it has to be acknowledged that the data on the organic fertilizers contains a non-quantified uncertainty. Further details on assumptions and calculations are given in Appendix A

Table 11: Determined variables and description of the farmer reported plant protection measures. The active substances and respective units were added based on expert knowledge (plant_protection.csv).

Column Name	Unit	Description
site	-	field name
date	YYYY-MM-DDThh:mm	application date
product	-	name of product
type	-	type of product: herbicide | fungicide | insecticide | growth control
dosage	-	amount applied in units specified in units
unit_dos	g ha^{-1}; L ha^{-1}	unit of dosage
act_subst_1	-	names of active substance in the product
unit_subst_1	g L^{-1}; g kg^{-1}	unit of act_subst1 in g kg^{-1} or g L^{-1}
act_subst_2	-	names of active substance in the product
unit_subst_2	g L^{-1}; g kg^{-1}	unit of act_subst2 in g kg^{-1} or g L^{-1}
act_subst_3	-	names of active substance in the product
unit_subst_3	g L^{-1}; g kg^{-1}	unit of act_subst2 in g kg^{-1} or g L^{-1}
comment	-	due to inconsistencies in units reported by the farmer, comments to the interpretations of the reports were added

Table 12: Determined variables and description of the weather data files (weather.csv).

Column Name	Unit	Description
site	-	field name
date	YYYY-MM-DDThh:mm	date of measurement
ws	m s-1	wind speed measured by a CSAT3 3D anomemeter
ws_flag	-	flag wind speed
wd	°	wind direction measured by a CSAT3 3D anomemeter (degrees against north)
wd_flag	-	flag wind direction
at	°C	air temperature measured 2 m above ground
at_flag	-	flag air temperature
rh	%	relative humidity measured 2 m above ground
rh_flag	-	flag relative humidity
ap	hPa	atmospheric pressure
ap_flag	-	flag atmospheric pressure
rs_down	W m-2	downwelling shortwave radiation (global radiation)
rs_down	-	flag downwelling shortwave radiation
rl_down	W m-2	downwelling longwave radiation
rl_down	-	flag downwelling longwave radiation
rs_up	W m-2	upwelling shortwave radiation (reflective radiation)
rs_up_f	-	flag upwelling shortwave radiation
rl_up	W m-2	upwelling longwave radiation
rl_up_f	-	flag upwelling longwave radiation
pr	mm	precipitation measured 1 m above ground
pr_flag	-	flag precipitation

Table 13: Determined variables and description of the eddy covariance measurement data files (flux_data.csv). For the variables nee_filtered, le_filtered, and h_filtered data points were removed according to the following rule: for the respective quality flag > 6 and those measured values which were > 5 times the median of the previous 4 days were discarded. The MPI REddyProc R tool was used to gap-fill and for partitioning net ecosystem exchange (nee) into ecosystem respiration and gross primary productivity

Column Name	Unit	Description
site	-	field name
date	YYYY-MM-DDThh:mm	date and time at the end of the 30-min averaging interval
nee	mmol m^{-2} s^{-1}	net ecosystem exchange of CO2
h	W m^{-2}	sensible heat flux
le	W m^{-2}	latent heat flux
rn	W m^{-2}	net radiation
shf1	W m^{-2}	soil heat flux in the 8 cm depth (heat flux plate 1)
shf2	W m^{-2}	soil heat flux in the 8 cm depth (heat flux plate 2)
shf3	W m^{-2}	soil heat flux in the 8 cm depth (heat flux plate 3)
ghf	W m^{-2}	ground heat flux: mean of shf1-3 plus change in soil heat storage (dS)
dS	W m^{-2}	change in soil heat storage in the 0 - 8 cm layer and between t_{i-1} and t_i (calorimetric method)
qf_ustar	-	[1]quality flag friction velocity (ustar), 1 - 9
qf_h	-	[1]quality flag sensible heat flux, 1 - 9
qf_le	-	[1]quality flag latent heat flux, 1 - 9
qf_nee	-	[1]quality flag net ecosystem exchange, 1 - 9
r_err_ustar	%	random error friction velocity
r_err_h	%	random error sensible heat flux
r_err_le	%	random error latent heat flux
r_err_nee	%	random error net ecosystem exchange
noise_ustar	%	instrumental noise friction velocity
noise_h	%	instrumental noise sensible heat flux
noise_le	%	instrumental noise latent heat flux
noise_nee	%	instrumental noise net ecosystem exchange
z_l	-	stability parameter
dir	°	wind direction (degrees against north)
ustar	m s^{-1}	friction velocity
nee_filtered	mmol m^{-2} s^{-1}	filtered net ecosystem exchange of CO$_2$
le_filtered	W m^{-2}	filtered latent heat flux
h_filtered	W m^{-2}	filtered sensible heat flux
tair_gf	°C	[2]gap-filled air temperature using REddyProc 1.2.2
vpd_gf	hPa	[2]gap-filled vapour pressure deficit using REddyProc 1.2.2
rn_gf	W m^{-2}	[2]gap-filled net radiation using REddyProc 1.2.2
nee_gf	mmol m^{-2} s^{-1}	[2]gap-filled net ecosystem exchange of CO$_2$
h_gf	W m^{-2}	[2]gap-filled sensible heat flux
le_gf	W m^{-2}	[2]gap-filled latent heat flux
reco	mmol m^{-2} s^{-1}	[3]ecosystem respiration partitioned from measured nee
gpp_f	mmol m^{-2} s^{-1}	[3]gross primary production partitioned from measured nee and simulated reco
reco_dt	mmol m^{-2} s^{-1}	[4]ecosystem respiration partitioned from measured nee
gpp_dt	mmol m^{-2} s^{-1}	[4]gross primary production partitioned from measured nee

[1]gap-filling algorithm and [2]partitioning algorithm both from Reichstein et al. (2005), [3]partitioning algorithm of Lasslop et al. (2010), [4]Foken (2006)

Table 14: Determined variables and description of the soil water content, temperature, heat storage and matric potential measurements. Partially, the research sites had different numbers of sensors of a given type. All had temperature sensors installed at 2, 6, 15, 30, and 45 cm soil depth, and matric potential and volumetric water content sensors installed at 5, 15, 30, 45, and 75 cm depth which are given separately in the individual files. For this reason, each data file (ec*_soil_data.csv) has its own metadata file.

Column Name	Unit	Description
site	-	field name
date	YYYY-MM-DDThh:mm	date of measurement
st	°C	soil temperature measurements
mp	kPa	matrix potential measurements
res	kOhms	resistance of the matrix potential sensors
vwc	$m^3\ m^{-3}$	volumetric water content
wtt	µSec	wave travel time of the vwc sensor
vwc_cal	$m^3\ m^{-3}$	site-specific calibrated volumetric water content
Cv	$J\ cm^{-3}\ K^{-1}$	soil volumetric heat capacity, calculated from the vwc in 5 cm dry bulk density
dT	K	change in near surface soil temperature, calculated from the arithmetic mean of the 2 cm and 6 cm soil temperature recordings of two successive half-hourly time steps, and computed differences of the mean.
dS	$W\ m^{-2}$	change in soil heat storage in the 0 - 8 cm layer between two half-hourly time steps, calculated calorimetrically from Cv and dT (de Vries, 1963)

[1] only reported for research sites EC1-3

Table 15: Variables and description of plant biomass file (biomass.csv).

Column Name	Unit	Description
site	-	field name
date	YYYY-MM-DDThh:mm	measurement date
plot	-	plot number of measurement
crop	-	growing crop
plant_no	m^{-2}	number of plants per square meter
tot_abv_bm	$g\ m^{-2}$	total above ground biomass: all plant tissues (stem + leaves) including generative biomass (grains) and glume or cob kernel and it's leaves
veg_bm	$g\ m^{-2}$	only vegetative, aboveground plant tissues: stem and leaves
gen_bm	$g\ m^{-2}$	grains; cob kernels; seeds
ear	$g\ m^{-2}$	ear weight
ear_no	m^{-2}	ear number
glume	$g\ m^{-2}$	glume weight
cob	$g\ m^{-2}$	cob weight
cob_no	m^{-2}	cob number per square meter
cob_leaves	$g\ m^{-2}$	cob leaves weight
tsw	$g\ 1000^{-1}$	thousand seed weight
res_wc_tot	%	residual water content (weight-%) of total biomass samples dried at 60 deg C
res_wc_veg	%	residual water content (weight-%) of vegetative biomass samples dried at 60 deg C
res_wc_glume	%	residual water content (weight-%) of glume biomass samples dried at 60 deg C
res_wc_gen_bm	%	residual water content (weight-%) of generative biomass samples dried at 60 deg C

Table 16: Variables and description of carbon and nitrogen content of the crop biomass (cn.csv).

Column Name	Unit	Description
site	-	field name
date	YYYY-MM-DDThh:mm	measurement date
plot	-	plot number
crop	-	growing crop
fraction	-	fraction of the crop the C and N percentages are related to : (straw = leaves and stem; generative = grains; total = (grains)+leaves+stem)
C	%	nitrogen content in the respective fraction's biomass
N	%	carbon content in the respective fraction's biomass

Table 17: Leaf area index measurement data and description of the LAI file (lai.csv).

Column Name	Unit	Description
site	-	field name
date	YYYY-MM-DDThh:mm	measurement date
plot	-	measurement plot number
crop	-	growing crop
lai_mean	$m^2\ m^{-2}$	arithmetic mean of the measurement plot's leaf area index
lai_sd	$m^2\ m^{-2}$	standard deviation of the measurement plot's leaf area index

5   **Table 18: Plant development stage and height measurement, and description of the phenology data file (phenology.csv).**

Column Name	Unit	Description
site	-	field name
date	YYYY-MM-DDThh:mm	measurement date
plot	-	plot number
crop	-	growing crop
replicate	-	number of measurement within the plot
bbch	bbch	bbch stage of the plant
plant_h	m	height of the plant

Table 19: Chamber flux measurements, the suffixes are identical to the ones in Table 9, as are the plot references, herein.

Column Name	Unit	Description
site	-	field name
date	YYYY-MM-DDThh:mm	measurement date
plot	-	plot number
co2	$kg\ C\ ha^{-1}\ hr^{-1}$	soil CO_2 evolution
instrument	-	instrument type
soil_temp	°C	soil temperature at measurement
ambient_temp	°C	ambient temperature at measurement
atmp	hPa	atmospheric pressure at measurement
sub_plot_type	-	"veg" - vegetated, and "b09", "b10", "b12" - bare plots in the years 2009, 2010, 2012